Differential Impacts of Hemin and Free Iron on Amoxicillin Susceptibility in *Ex vivo* Gut Microbial Communities

By

Francesco Pagano

BS Biology, Rensselaer Polytechnic Institute, 2019

Thesis

Submitted in partial fulfillment of the requirements for the Degree of Master of Science in the Graduate Program of Biotechnology at Brown University

PROVIDENCE, RHODE ISLAND

MAY 2025

AUTHORIZATION TO LEND AND REPRODUCE THE THESIS

As the sole author of this thesis, I authorize Brown University to lend it to other institutions for the purpose of scholarly research.

Date: April 01, 2025

Francesco Pagano, Author

I further authorize Brown University to reproduce this thesis by photocopying or other means, in total or in part, at the request of other institutions or individuals for the purpose of scholarly research.

Date: April 01, 2025

Francesco Pagano, Author

This thesis by (Francesco Pagano) is accepted in its present form by the Graduate Program in Biotechnology as satisfying the thesis requirements for the degree of Master of Science

Date_____ Signature: _____

Dr. Peter Belenky, Advisor

Date_____ Signature: _____

Dr. Karthikeyani Chellappa, Reader

Date_____ Signature: _____

Dr. Anita Shukla, Reader

Approved by the Graduate Council

Date_____ Signature: _____

Dr. Thomas Lewis, Dean of the Graduate School

Acknowledgements

I would like to take this opportunity to thank the Brown University Biotechnology MS Program; my time as part of this program has been transformative and eye opening. During my time here, I have developed particular confidences in my research and a drive for challenge. To that end, I would like to thank Dr. Jacquelyn Schell for her guidance throughout the program.

I would like to express my sincere gratitude to Dr. Peter Belenky for his support and guidance through my time in the Biotechnology Master's Program and for helping me navigate the realm of microbiology research. I would also like to thank Dr. Swathi Penumutchu and Rachel Peterson for their invaluable help in training me during my formative months working in the Belenky Lab. I would also like to thank all the members of the Belenky Lab for their constant support and assistance throughout the years: Noelle Curtis-Joseph, Melanie Ortiz Alvarez De La Campa, Dr. Rachael Nilson, Rachel Peterson, Dr. Swathi Penumutchu, Devin Bemis, Dr. Stephen Costa, Dr. Chapman Beekman, Audra Laubi, and Casidhe Hughes.

I would also like to thank Dr. Rahiya Rehman and Dr. Jason Shapiro for allowing us to use their samples for generation of preliminary data to validate our pipeline. I would also like to take time to thank my committee members Dr. Anita Shukla and Dr. Karthikeyani Chellappa for their time.

This work was supported by grants from the National Institute of Diabetes and Digestive and Kidney Diseases (R01-DK125382), the National Center for Complementary and Integrative Health (R56-AT012463), and the National Institute of Food and Agriculture (2020-67017-31697).

Table of Contents

Table of Figures

Table of Tables

Abstract of Differential Impacts of Hemin and Free Iron on Amoxicillin Susceptibility in Ex vivo Gut Microbial Communities, by Francesco Pagano, SCM, Brown University, 01 May, 2025

Objective: The rise of antibiotic resistance infections worldwide has created a need to enhance the efficacy of existing antibiotics. Modification of metabolism has been shown to potentiate antibiotic lethality. In this study, we employed a novel *ex vivo* approach to culture microbial communities to study the effects of different forms of iron on amoxicillin susceptibility. **Methods:** Communities, ranging from known synthetic communities to complex unknown human stool microbiome samples, were cultured out and treated with amoxicillin and had their optical densities monitored. These samples were sequenced using an Oxford nanopore long read 16S rRNA V4-V9 approach and computationally defined using the Emu algorithm. The validity of this pipeline was confirmed along consortia, murine cecal content, and clinically relevant patient stool samples. Commercially available stool samples were then treated with between 0 and 75 μM hemin, $FeSO_4$, or $FeCl_3$ for 24 hours alongside amoxicillin (0 – 10 μg/mL) and profiled to identify the effects of different forms of iron on amoxicillin susceptibility. **Results:** Alpha diversity, beta diversity, and normalized relative abundances confirmed the efficacy of the selected *ex vivo* pipeline, allowing for ~ 77%% species retention over 24 hours. Treatment of communities with hemin protected *Bacteroides, Escherichia-Shigella, Parabacteroides,* and *Parasutterella* against amoxicillin. Two forms of free iron matched to this concentration did not protect these genera from amoxicillin. **Conclusions:** This study shows that the *ex vivo* protocol successfully generates large reproducible data for studying the effects of metabolic modulators on antibiotic susceptibility. Genera protected against killing through hemin supplementation are efficient in iron sequestration and produce large siderophore

numbers. In the future, metatrascriptomics should be employed in future studies to identify common metabolic mechanisms of hemin-induced protection. This mechanistic understanding may lead to hemin-based therapies to modulate antibiotic efficacy in the host.

Chapter 1: Introduction

1.1 The Microbiome & Human Health

The microbiome can be defined as the collection of all microorganisms within a distinct environment as well as their genetic material and sphere of activity.[1] Microbiomes exist in various major sites throughout the human body, including the skin, gastrointestinal (GI) tract, oral cavity, lung, and vaginal tract, and vary differently in their makeup from site to site.[2] The GI tract alone is believed to house over 10^{14} microorganisms[3] and hundreds of species.[4] Microbiomes vary from person to person drastically, and are influenced by multiple factors such as age, antibiotic usage, genetics, early life feeding practices, and dietary habits.[5] Because of this, there is no defined gut microbial composition that is considered healthy; rather, the metabolic functions define healthy microbiomes.[6]

The microbiome of the GI tract performs a variety of functions: the production of short chain fatty acids (SCFAs), the breakdown of complex nutrients for host use, synthesis of various bioactive molecules, the production of antimicrobial substances to inhibit infection, and development of the immune system.[2, 7-11] Bacteria growing in the GI tract are influenced by a multitude of factors. Along the GI tract, pH, oxygen, and nutrient availability drastically change, creating environmental niches alongside the length of the tract;[12-15] as such, certain species of bacteria thrive more effectively within certain sections of the gut.[16, 17] Oxygen concentrations, in particular, drastically decrease along the length of the intestinal tract, leading to physiologically anaerobic conditions within parts of the large intestine, cecum, and colon.[18] The anaerobic nature of these sections of the GI tract lead to unique bacterial niches. The anaerobic bacteria that colonize these areas are implicated in a variety of important functions that assist in

establishing homeostasis, such as the breakdown of host-undigestible nutrients, starch fermentation, and the production of short chain fatty acids.[19, 20]

When these environments are disturbed, however, dysbiosis is established in these regions. Dysbiosis can be briefly defined as a shift in the microbial diversity, composition, and load away from established normal levels, changing the metabolic output of the microbiome.[21] Dysbiosis can be caused by major shifts in diet, xenobiotics, infections, and inflammation.[22] High fat high sugar diets, commonly referred to as the Western diet, can alter the makeup of the microbiome and promote the growth of Proteobacteria.[23, 24] Xenobiotics such as antibiotics are extremely effective at causing dysbiosis, sometimes termed antibiotic-induced dysbiosis (AID), and can drastically reduce microbial diversity and bacterial load.[25] Changes in the microbiome in the short term can lead to acute complications such as diarrhea[22, 26] and increase the possibility of infection.[27] Dysbiosis has also been associated with other diseases such as irritable bowel disease and diabetes.[27] Microbial interventions to alleviate dysbiosis as a treatment strategy have gathered attention in recent years in the biotech industry. The use of fecal microbiota transplants, particularly, to treat severe infections such as recurrent *Clostridoides difficile* infections has seen recent success in years.[28]

1.2 Studying Microbial Composition

In order to ascertain the role of microbes and microbial composition on host health, comparison studies have been performed to look at the makeup of the microbiomes of certain sections of the gut. These studies are traditionally performed using one of two methods: 16S rRNA amplicon sequencing, or shotgun metagenomics. 16S rRNA amplicon sequencing

employs the principle of sequencing the highly conserved 16S rRNA gene in bacteria, which spans 9 hypervariable regions containing many single nucleotide polymorphisms that can be used to map to specific taxa.[29] 16S rRNA gene amplification approaches generally amplify a 200-300bp product of one or two hypervariable regions, most commonly the V4 and/or V5 regions,[30] from genomic DNA collected from biological samples and sequence them on the Illumina MiSeq platform. The Illumina 16S rRNA gene amplification and taxonomic discerning pipelines are highly optimized for an easy and cheap analysis to gain taxonomic information. This approach, however, cannot distinguish between species of the same genus particularly well, leading to a lack of understanding of sample makeup at the species level.

Shotgun metagenomics fragments gDNA and analyzes microbial composition by aligning detected reads against a microbial database that includes the entire genetic information for multiple organisms.[31] Because of this approach, alignment using the entire genome to taxonomic databases[32] allows for more accurate species information, and allows for clarity down to the strain level. Shotgun metagenomics also allows for functional analysis of the entire gDNA to gain community-level functional knowledge.[33] Library preparation and sequencing per sample costs, however, tend to be much higher comparatively due to sequencing depth required to achieve sufficient organism coverage, and the pipeline is generally computationally taxing to perform in order to gain high end results. Another limitation of shotgun metagenomics is that reads without a reliable reference in the database do not get characterized.

The development of third generation sequencers, primarily dominated by PacBio and Oxford Nanopore Technologies (ONT) since their introductions in the early 2010s, allowed for the sequencing of long reads without the need for PCR amplification.[34] The ONT sequencer MinION uses a nanopore to serve as a sensor against single stranded DNA to detect nucleotides

in real-time through changes in electrical current.[35] This has allowed labs to perform whole genome sequencing on microbial samples,[36] as well as sequencing long read versions of the 16S rRNA gene for genus and species level taxonomic classification.[36, 37] The Nanopore sequencing process, however, is error-prone,[38] and thus there is a need for an a software or algorithm to account for the high errors produced from sequencing reads. One such software that tackles this error-prone nature is Emu, which is a microbial community profiler that first aligns reads to a reference database then uses an expectation-maximization algorithm to predict errors and reduce their impact down to the species level.[39]

Microbial composition analysis and the impact stimuli may have on microbial communities is currently studied under the context of *in vitro* synthetic communities, stool samples from animals or patients, or *in vivo* contents from animals; each of these sample types have their own benefits and drawbacks. Synthetic communities that mimic the functional capacities of *in vivo* communities are relatively easy and cheap to maintain, and allow for real time monitoring of bacterial growth and the ability to test a myriad of conditions with quick turnover.[40-43] These communities do not completely encompass the metabolic and functional capacity of *in vivo* communities, and therefore struggle in certain aspects of animal and human translatability. Stool samples collected from patients allow for snapshots of the microbiomes of the colon at different timepoints and are easy to collect and more closely model the internal microbiomes of animals and humans, but are not perfect in their representation of their entire GI tract. *In vivo* studies provide the most translatable information on microbial makeup and how this may affect host health; the collection of this form of sample, however, is substantially more invasive and may require sacrifice of the animal model.[44] These sample types do not represent the human microbiome in its capacity and cannot recapitulate the complexity of microbial-

immune system interactions taking place in humans. Samples obtained from humans and animals also require large numbers of individuals for accurate results, which can lead to drastic increases in cost.

The development of *ex vivo* culturing methods has been relatively successful in creating results that closely resemble host microbiomes by culturing samples under anaerobic conditions that allow for monitoring of bacterial growth and response to agents and stimuli. These techniques, however, require passaging multiple times, leading to stable community stocks that are statistically different than their starting makeup, reducing the translatability of these results.[43, 45-49] There is also no universally agreed upon media for cultivation of communities, as many medias produce cultures biased to a group of members as not all bacteria grow equally well in the same media, and some may not grow at all.[50] Modified Gifu Anaerobic Media (mGAM) is a relatively successful media that is used to culture a large number of microbes spanning various phyla, and has been used to establish stable synthetic communities[51] and grow *ex vivo* samples from mice.[46] mGAM uses a higher ratio of fibers to simple sugars, digested proteins, host factors and hydrogen acceptors through sodium thioglycolate and L-cysteine to support growth of anaerobic microbes.[52, 53] The supplementation of mGAM with other components can be used to support the growth of other microbes that may not otherwise be supported.

1.3 Antibiotics & The Role of Metabolism in Antibiotic Susceptibility

Antibiotics are one of the most commonly prescribed class of drugs in the US, and constitute over 200 million prescriptions a year to treat infections.[54] Antibiotics range in their function and efficacy against specific microbes; bacteriostatic antibiotics act through inhibition

of growth, while bactericidal antibiotics eliminate bacteria in an active manner.[55] Since the initial discovery of penicillin in 1928 by Alexander Fleming,[56] many classes of antibiotics from various sources have been discovered. Some of these classes include aminoglycosides and tetracyclines, which target ribosomal subunits; glycopeptides, cephalosporins, carbapenems and penicillins, which target cell wall synthesis; and fluoroquinolones, which target DNA synthesis.[57-64] Of these, amoxicillin is the most commonly prescribed antibiotics in the United States.[54] Amoxicillin is a broad-spectrum antibiotic of the penicillin group and operates through targeting penicillin-binding proteins to inactivate and shut down synthesis of peptidoglycan, leading to lysis and cell death.[65, 66] Amoxicillin is clinically used to treat a myriad of infections, including those caused by *Streptococcus* species, *H pylori*, *Pneumococcus* species, *E faecalis*, and *E coli.*[67-72]

Due to the overprescription of antibiotics over the years, strains of bacteria that are resistant to different classes of antibiotics have arisen. In 2019 alone, 4.95 million deaths occurred globally as a result of drug-resistant infections.[73] Patients are affected not only through increased risk of mortality and morbidity from direct infection but also from a change in medical practice that may result from an inability to utilize antibiotics either prophylactically or clinically in many routine medical procedures.[25, 57, 73] In order to overcome increasing rates of antibiotic infections and the rise of more serious antibiotic-resistant infection, it is important for the scientific community to identify ways to make antibiotics more effective against various microbial infections.

One such avenue to modify antibiotic susceptibility of microbes and communities has been through modifying metabolism. Over the past 15 years, it has been identified that modifying the metabolic flux in bacteria can drastically affect the killing efficacy of antibiotics.[73]

Early work in the field identified that genetically modifying *E. coli* to increase their basal respiration aerobically led to an increase in antibiotic susceptibility to ampicillin;[73, 74] this phenomena in part may be due to an increase in oxidative stress.[75] This observation is further supported with the observation that *B. thetaiotaomicron* blooms in response to amoxicillin and upregulated complex sugar utilization.[76] Anaerobically *in vitro*, *B. thetaiotaomicron* becomes more sensitive to amoxicillin when fed glucose, and is protected against amoxicillin when supplemented with pectin; when grown in media with both glucose and pectin, however, the effects of glucose dominate and amoxicillin susceptibility was increased.[76, 77] In more complex communities *in vivo*, high fiber diets reduced dysbiosis as a result of amoxicillin treatment compared to standard diets, and glucose exacerbated antibiotic-induced dysbiosis through blooms in Proteobacteria.[78] Metabolically, it was identified that glucose increased oxidative metabolism while fiber repressed this increase in oxidative metabolism.[78] Work conducted in *E. coli* indicates that the beta-lactam-induced metabolic burden results from a futile cycle of peptidoglycan synthesis to degradation, and that removing this activity through direct inhibition or the reduction of ATP synthesis results in reduced toxicity.[66, 74, 75] Knowing this, it stands to reason that overloading the electron transport chain to force microbial communities into futile cycling can potentiate the response of microbes in complex communities to antibiotics.

Iron is an essential metal for most living organisms. Iron can exist in a ferric (Fe^{3+}) or ferrous (Fe^{2+}) form, as well as can be parts of cofactors involved in various biological processes.[79, 80] One such way that iron is able to react within its environment is through the Fenton reaction, where ferric or ferrous iron can react with hydrogen peroxide to produce hydroxyl radicals that are highly reactive.[81] This production of hydroxyl radicals are highly reactive with DNA, and have been shown to kill many cell types through DNA strand

breakage.[82-84] The Fenton reaction can also occur anaerobically at lower efficiency,[85] and iron reactions have been shown to be able to participate in nitrate reduction through iron oxidation in anoxic conditions.[86] Anaerobically, ferric iron can act as a terminal electron acceptor in the electron transport chain to help produce ATP.[87, 88] The role iron may have in antibiotic susceptibility has been explored, though results are conflicting. Traditional approaches used to look at the role of iron in antibiotic susceptibility include the addition of a known concentration of iron to media or the addition of an iron chelator to remove iron from media.[89] Depending on the approach, results are conflicting in nature; for example, the removal of iron from the media was found to cause a decrease in *E. coli*'s resistance to clindamycin, mupirocin, tetracycline, and clarithromycin, while approaches using chelators found that decreasing iron lead to an increase in resistance to cephalosporin, ampicillin, chloramphenicol, methicillin, and vancomycin while having no effect on susceptibility to erythromycin, spectinomycin, chloramphenicol, rifampicin, and tetracycline.[89-94] Other species such as *P. aeruginosa* show similar conflicting results. The addition of iron to media caused reduced resistance to ampicillin, norfloxacin, gentamicin, ofloxacin, and cefsulodin; the opposite was also observed, however, where addition of iron has also caused increased resistance to tobramycin and tigecycline.[89, 95-97] In complex communities *in vivo*, oral supplementation with iron sulfate through diet post-antibiotic exposure lead to an initial decrease in alpha diversity and has been found to lead to an increase in *Parasutterella* and *Bacteroides* genera.[98] The particular role that many other forms of iron like hemin on complex microbial communities has yet to be elucidated. In this study, we propose a novel culturing pipeline that allows us to monitor the role various forms of iron have on antibiotic susceptibility in complex communities *ex vivo.* The relationship iron in its ferric form, ferrous form, and as part of a cofactor with amoxicillin was evaluated through this pipeline, allowing for the

identification of four unique genera protected against amoxicillin killing in response to increased hemin, and not free iron, in media.

Chapter 2: Methods

2.1 Media Preparation

Minimal Gifu Anaerobic Broth Media (mGAM) (Hyserve 1005433) was prepared per manufacturing instructions; briefly, 41.7g was suspended per liter of H_2O and heated to allow to dissolve before autoclaving at 121°C for 15min. All mGAM was supplemented with 1m of mucin (Sigma-Aldrich M1778) prior to autoclaving to allow for dissolving. Media was placed in anaerobic chamber at least 24 hours in advance to experimentation to allow for exchange of gases. Desulfovibrio Postgate Medium (DPM) was prepared using a modified version of a DSMZ established protocol;[99] briefly, Solution A (0.5g/L K_2HPO_4, 1.0g/L NH_4Cl, 1.0g Na_2SO4, 0.1g $CaCl_2$ x $2H_2O$, 2.0g $MgSO_4$ x $7H_2O$, 2.0g Na-L-lactate, 1.0g Yeast extract, 980mL H_2O), Solution B (0.5g $FeSO_4$ x $7H_2O$, 10mL H_2O), and Soluction C (0.1g Sodium thioglycolate, 0.1g Asocrbic acid, 10mL H_2O), were prepared while spinning. Solution A was filter sterilized using a 0.22 μm bottle vacuum filter (Corning 430015) using sterile flame technique followed by autoclaving at 121°C for 15min, and Solutions B and C were filter sterilized using 0.22 μm centrifuge tube filters (Millipore SCGP00525) by sterile flame technique. Solutions B and C were added to room temperature Solution A and immediately placed in anaerobic chamber and allowed to exchange gases. Working media for culturing (10%DPM/mGAM+mucin) was created by diluting a ratio of 1mL DPM in 9mL of mGAM + 1mg/mL mucin) using sterile flame techniques.

2.2 Anaerobic Chamber Conditions

A Coy Lab Products vinyl anaerobic chamber (Coy Labs 7150000) was used to create anaerobic conditions for all cultures and culturing conditions. The vinyl anaerobic chamber is outfitted with an incubator (Coy Labs 6100000) set at 37°C, a recirculating HEPA atmospheric filtration system (Coy Labs 8537025V), an anaerobic gas infuser (Coy Labs 8100110) and a dehumidifier (8533110) to ensure anaerobic conditions. The chamber is also outfitted with an anaerobic monitor, model 12 (Coy Labs 6250000) to allow for monitoring of anerobic conditions and hydrogen % content. Atmospheric makeup of the machine is created using a mixture of two gases: pure nitrogen gas, and a mixed gas containing 5% CO_2, 5% H_2, and balance N_2. Gases are mixed into the chamber to obtain a 2.0-2.5% hydrogen content, and an O_2 = 0-10 ppm.

2.3 Establishment of Consortia

Eight bacterial species were chosen to create a synthetic community: *Akkermansia muciniphila, Bacteroides fragilis, Bacteroides thetaiotaomicron, Bifidobacterium longum, Desulfovibrio desulfuricans, Escherichia coli, Lactobacillus johnsonii,* and *Roseburia hominis.* Please see Table 1 for information on bacteria species and vendor. All species, except for *D. desulfuricans* and *B. longum*, were grown in 5mL mGAM +1mg/mL mucin media for 24 hours, with the two exceptions being grown in 5mL DPM for 48H. 150µL of culture were plated and diluted with equal parts sterile filtered PBS, and OD_{600} measurements were taken using the Molecular Devices SpectraMax M3 Spectrophotometer using SoftMax Pro v6, blanking the culture to its original medium. Cultures were then consolidated in the following ratios in 10% DPM/mGAM + 1mg/mL mucin to achieve an OD_{600} of 0.1: 1 part each *B. thetaiotaomicron, B.*

fragilis, E. coli, and *B. longum* to 5 parts each *R. hominis, L. johnsonii, D. desulfuricans,* and *B. longum*. Consortia was then run through downstream sequencing protocol.

2.4 Collection of Mouse Cecal Content into Chamber

Cecums from male C57BL/6J mice (Charles River) were collected; in brief, mice were anesthetized via isoflurane, followed by cervical dislocation per the approved IACUC protocol 23-05-0013. Mice were then dissected, and the entire intestinal tract was collected into a sterile plate and transferred to the anaerobic chamber. In the anaerobic chamber, the cecum was isolated from the rest of the GI tract and its contents (approximately 200 μL) were transferred into approximately 15 mL of 10% DPM/mGAM + 1mg/mL mucin media and cultured for approximately 2H. After 2 hours, cultures were treated (see section 2.6 for further details).

2.5 Human Material Processing

For human communities used to verify protocol, human stool samples were obtained through an active research collaboration between the Department of Molecular Microbiology and Immunology at Brown University and the Pediatric Inflammatory Bowel Disease Center at Hasbro Children's Hospital (IRB 1930822-3) by Rahiya Rehman, and immediately frozen at -80°C. Approximately 130 mg of stool samples were weighed out and placed into 20mL of 10%DPM/mGAM + 1mg/mL mucin, pipetted to break up the matter, and grown for 24 hours while shaking at ~400rpm. Cultured content was then frozen at -80°C in 1mL aliquots in 20% filtered glycerol (Fisher Sci G331) until the start of the experiment. On the day of the

experiment, frozen cultures were diluted 1:200 in media prior to the start of the experiment (see section 2.6 for further details).

For cultures treated with iron and amoxicillin, human stool samples were obtained through vendor BioIVT (BioIVT HUMANFECES-0000263); donor information was deidentified prior to receival of material. Samples upon arrival were immediately frozen at -80°C. Approximately 130mg of stool samples were weighed out and placed into 20mL of 10%DPM/mGAM + 1mg/mL mucin, pipetted to break up matter, and grown until exponential growth phase for 5 hours while shaking at ~400rpm. Content is then frozen at -80°C in 1mL aliquots in 20% filtered glycerol (Fisher Sci G331) until the start of the experiment. On the day of the experiment, frozen culture content is diluted 1:200 in media and allowed to grow until once again at the exponential growth phase (~6 hours) before treatment (see section 2.6 for further details).

2.6 *Ex vivo* Culturing of Microbial Samples

Input cultures, prior to plating, were first grown to exponential phase before treatments. Cultures were then treated with hemin (Fisher Sci AAA1116503), $FeSO_4$ (Sigma-Aldrich F8633) or $FeCl_3$ (Fisher Sci AC169430050), and are then plated 300 µL/well in a 96 well flat bottom plate (Corning 3370) and treated with amoxicillin (Millipore A8523) at concentrations of 50 µg/mL, 10 µg/mL , 12.5 µg/mL, 3.125 µg/mL, 2µg/mL, or 0 µg/mL using amoxicillin stocks diluted in DMSO (Fisher Sci BP2311). Cultures' optical densities are monitored for 24H using the Cerillo Alto Kinetic Microplate Reader while incubating at 37°C in the anaerobic chamber and cultures are collected at 24 hours post treatment for downstream applications.

2.7 DNA Cleanup

Cultures collected post treatment are processed via a selected portion and kit of an established protocol from ZymoResearch (Zymo D4310). Briefly, 300 μL of sample were centrifuged at 2250xg for 8 minutes to pellet the sample and supernatant is removed. A DNase enzyme (Zymo D4310350) was added in buffer (Zymo D431025) to the pellet, vortexed, and incubated for 15min at 37°C. Samples were then treated with a Proteinase K (D30012125), vortexed, and incubated at 55°C for 10min, and diluted in DNA/RNA Shield (R1100250) 1:1 and frozen at -80°C until further use.

2.8 *E. coli Nissle* Spike-In & DNA Cleanup Test on Synthetic Community

E. coli Nissle 1917 (see Table 1 for more information) was grown to stationary phase in mGAM + 1 mg/mL mucin then diluted to an OD_{600} of 0.5. These *E. coli* cultures were then treated for 30 minutes with amoxicillin (Millipore A8523) at a concentration of 100 μg/mL and then mixed 1:1 into the synthetic communities derived from Section 2.3 that were also mixed to a final OD_{600} of 0.5 before. These spiked communities were then treated with or without the DNA Cleanup step detailed in Section 2.7 and had their 16S rRNA gene amplified and sequenced as outlined in section 2.9.

2.9 16S rRNA Amplification Prep and Sequencing

DNA for all samples was extracted using the ZymoBIOMICS Quick-DNA Fecal/Soil Microbe 96 Kit (Zymo D8011) following manufacturer instructions. Total DNA was eluted into nuclease-free water and quantified using the dsDNA-BR kit on a Qubit 4.0 fluorometer

(ThermoFisher Scientific, Waltham, MA, USA) before use in downstream amplicon and library preparations.

16S rRNA V4-V9 hypervariable regions were amplified from total DNA using barcoded 515F forward primers from the Earth Microbiome Project[30] and using a matched set of reverse barcodes alongside the 1492R primer. See Table 2 for reverse barcoded primer sequences used. Amplicons were created using 5X Phusion HF DNA Polymerase (Fisher Sci F530L) under the following PCR conditions: an initial denaturation at 98°C for 30s followed by 25 cycles of 98°C for 10s, 57°C for 30s, and 72°C for 30s. Amplicons then underwent a final extension at 72°C for 5 min. Amplicons were visualized for confirmation of successful amplification via gel electrophoresis, and pooled at equal DNA weight before PCR cleanup using Macherey-Nagel Gel and PCR Clean-Up kit (Macherey-Nagel 740609.250) per manufacturer specifications. Amplicons then underwent library preparation and secondary barcoding and run on the Nanopore MinION MK1B (ONT MIN-101B) per manufacturer instructions using the Native Barcoding 24 v14 kit (ONT SQK-NBD114-96).

2.10 Coding Pipeline

16S rRNA sequences were first basecalled using Nanopore's Guppy Software v6.5.7 through the guppy_basecaller function. These reads were then demultiplexed using Nanopore's Guppy Software v6.5.7 using the guppy_barcoder function, and barcodes and adapters were trimmed. Primary demultiplexed reads were then secondarily demultiplexed using Porechop with custom barcode inputs denoted from the Earth Microbiome Project[30] and Table 2. Taxonomic assignments were performed along the SILVA database[32] using Emu.[39] Alpha

diversity (Shannon Diversity) and beta diversity (Bray-Curtis dissimilarity) were performed using the phyloseq package v1.46.0[100] in RStudio v12.1.[100, 101]

2.11 Percent Survival Determination

Bacterial species denoted in Table 1 were grown in mGAM + 1mg/mL mucin for 24 hours prior to experiment anaerobically. Bacterial species were then treated then diluted 1:1000 in media containing no iron or supplementations of different concentrations of hemin (Fisher Sci AAA1116503), $FeSO_4$ (Sigma-Aldrich F8633) or $FeCl_3$ (Fisher Sci AC169430050), and are then plated 150 μL/well in a 96 well flat bottom plate (Corning 3370) with the top row receiving 285 μL of inoculated bacteria; the top row is then treated with amoxicillin (Millipore A8523) to a starting concentration of 250 μg/mL to a total volume of 300 μL before serially diluting at a ratio of 1:1 to achieve a concentration range of 0 – 250 μg/mL. Plates are then incubated at 37°C for 20 hours before diluting 1:1 with 1XPBS (Fisher Sci BP39920) and OD_{600} measurements were taken using the Molecular Devices SpectraMax M3 Spectrophotometer using SoftMax Pro v6. Percent growth was then calculated against 0 μg/mL treated cultures, and Gompertz Equation for MIC Determination was employed to determine MIC_{90} using Prism GraphPad v10.4.1.

2.12 Statistic Analyses and visualizations

Specific details pertaining to statistical analyses for all experiments are detailed in the figure legends and results section. All sample numbers represent technical replicates. MaAsLin2[102] was used to analyze outputs from Emu. Statistical T tests and Gompertz Equation

for MIC Determination were performed in Prism GraphPad v10.4.1. All other graphs were created using Prism GraphPad v10.4.1.

Chapter 3: Results

3.1 An *Ex Vivo* Culturing Approach Allows for the Successful Cultivation and Sequencing of a Synthetic Consortia Community and Murine Cecal Communities

To properly discern the effects of various sources of iron on microbial communities while reducing the use of mice, we developed and validated an *ex vivo* protocol to study the microbiome. *Ex vivo* culturing techniques have been used in the past to identify changes in the microbiome,[43, 45-47] but a significant drawback of these techniques is the large number of passages that, though stabilizing the microbiome, cause the passaged communities to differ substantially from original community inputs.[48, 49] A protocol is thus necessary for cultured communities to better resemble the original communities in question. A brief overview of the protocol developed is seen in Figure 1A. Known synthetic bacteria communities and unknown human stool microbiome samples were cultured for 24 hours and treated with amoxicillin, with their optical density monitored. The cultured samples then have their 16S rRNA V4-V9 region amplified using a double barcoding approach modified from the Earth Microbiome Project[30] and run on the Nanopore MinION and demultiplexex and aligned using the Emu algorithm. [39] The Emu algorithm was used for in taxonomic alignment to more accurately discern species taxonomic information and overcome the more naturally error prone results of the Nanopore.

To test the validity of this pipeline, we cultured a synthetic community containing eight microbial species combined to act as the initial community input for the pipeline: *A. muciniphila, B. fragilis, B. thetaiotaomicron, B. longum, D. desulfuricans, E. coli, L. johnsonii,* and *R. hominis*. These microbes were chosen to represent a wide range of phyla, and more information on these species can be found in Table 1. When this community was treated with 10 μg/mL amoxicillin for 24 hours, there was a noticeable increase in the relative abundance of *E. coli* in

the community (Figure 1B). Because the community was treated for 24 hours with a bactericidal drug, it was possible that DNA from dead microbes, including *E. coli* could be represented downstream in the taxonomic abundances. To reduce the impact of DNA from killed microbes, we chose to use a DNA cleanup step comprising of a DNase treatment followed by a Proteinase K treatment prior to DNA extraction. To test this step, we spiked our synthetic community with an equal OD_{600} of *E. coli* killed with 100 μg/mL of amoxicillin for 1 hour and treated with or without the DNA cleanup steps to eliminate free floating DNA (Figure 1C). Treating the community with the DNA Cleanup alone caused a limited shift in the relative abundance of the community and a general reduction in the relative abundance of *E. coli*. When a mixture of dead and viable *E. coli* was spiked into the base community, *E. coli* dominated the overall relative abundance as expected. Performing a cleanup on this "spike-in" community reduced the abundance of *E. coli* to mirror the community that had not been spiked with killed *E. coli,* indicating that the proposed cleanup was effective at eliminating killed bacteria.

While this cleanup step worked well for a known synthetic community, we still needed to confirm its effectiveness for mammalian samples. Additionally, we needed a way to compare relative abundance with the overall growth of the culture. In order to accomplish this, murine cecal samples were collected to be used as the complex community input detailed in Figure 1A and treated with different amoxicillin concentrations for 24 hours followed by the presence/absence of our DNA Cleanup step prior to amplification and sequencing (Figure 1D). Data generated from the pipeline was normalized to OD_{600} to integrate overall community growth with the relative abundance data. Treatment of the communities with amoxicillin created a stepwise reduction in total normalized relative abundance of the murine cecal samples. The implementation of the DNA cleanup step showed changes in a few families of bacteria within the

communities. Families in bold reduce in normalized relative abundance as a result of the DNA cleanup, indicating that these families are overrepresented and experience more drastic killing as a result of the culturing and antibiotic treatment; these families identified include Anaerovoracaceae, Bacteroidaceae, and Enterobacteriaceae. Families underlined indicate an increase in normalized relative abundance as a result of the DNA cleanup, indicating that these families are normally underrepresented without it; these families include Acholeplasmataceae, Akkermansiaceae, Butyricicoccaceae, Desulfovibrionaceae, Lactobacillaceae, and o_Clostridia UCG-014.

3.2 *Ex Vivo* Culturing Pipeline Successfully Cultures Bacteria in Clinical Human Stool Samples Over a 48 Hour Period

The pipeline was also tested using clinically relevant patient stool samples obtained from a collaborator at Hasbro Children's Hospital that were cultured and frozen in 20% glycerol to act as starting communities in the pipeline. The overall alpha diversity, depicted in Figure 2A through Shannon diversity, indicates that the patient donor stool sample contained a Shannon diversity of 3.25. When cultured out for 24 hours and frozen, these samples retained a Shannon diversity that was similar to that of the initial stool sample, and further culturing of the samples out to 48 hours reduced the variance of the culture while also not significantly altering the Shannon diversity over these 24 hours. The variance between samples plotted using Bray-Curtis beta-diversity (Figure 2B) showed similar and close clustering of the three groups in terms of their similarity/dissimilarity, leading to the conclusion that culturing out the microbiome for up to 48 hours did not have a significant change on the overall diversity of the samples. A closer look at the abundance makeup of the communities, shown in Figure 2C, shows shifts in a few

families as a result of culturing, though the communities as a whole are once again not drastically different; Bifidobacteriaceae, Sutterellaceae, and Tannerellaceae increase as culturing times are increased, while Muribaculaceae increase, then decrease over the 48-hour time frame.

In order to identify species retention over time of these samples, a "Percent of Species Still Present from Baseline" value was calculated (Figure 2D), where the percentage of species that retained at least 1% of their relative abundance values compared to the donor stool sample was identified. Culturing of the stool sample for 24 hours allowed for a 1% species retention threshold of about 77%, while culturing the communities further out to 48 hours resulted in a 1% species retention threshold of 43.25%. This data particularly highlights the effectiveness of the culturing portion of the pipeline to retain species over time; it should be noted that increasing total culturing times begins to cause a degradation in the total number of species represented, so special care should be taken to reduce total culturing time.

3.3 Hemin protects four genera against Amoxicillin-Induced Death

Iron is a critical factor in bacterial metabolism, and previous research has shown that it may influence antibiotic efficacy.[89, 98] Given that human-derived components are a major source of iron in mGAM media, we selected hemin as a potential modulator of antibiotic lethality. Since iron can serve as a terminal electron acceptor in metabolic processes and anaerobic respiration, [88, 103] we hypothesized that altering hemin concentrations within the media could push microbial communities toward a more energy-productive state, thereby enhancing antibiotic lethality. To test this hypothesis, we used a human microbiome biospecimen obtained from BioIVT as the input community.

We found that hemin supplementation alone slightly reduced the initial growth rate of the microbiome culture but ultimately resulted in a higher final OD_{600}. When combined with 2 μg/mL or 10 μg/mL amoxicillin, hemin had a modest effect on early culture inhibition kinetics but led to higher final ODs compared to antibiotic treatment alone. This suggests that hemin facilitates microbiome recovery following initial AMX inhibition, potentially aiding post-antibiotic microbiome restoration or supporting bacterial survival in the presence of antibiotics.

We sequenced this community and first profiled alpha diversity at 24 hours, finding that AMX led to the expected significant drop in Shannon diversity in both the + 0 μM and + 15 μM hemin groups (# $p < 0.05$). On the other hand, the + 60 μM hemin cultures started with a significantly lower Shannon diversity (* $p < 0.05$) without amoxicillin treatment compared to the + 0 μM hemin group and exhibited no significant changes in Shannon diversity as a result of amoxicillin treatments (Figure 3B). The Bray-Curtis dissimilarity beta diversity plot of the samples showed distinct concentration-driven separation along PC2 for amoxicillin either at zero or 15 μM hemin (Figure 3C). The presence of 60 μM hemin shifted the community into the positive PC1 quadrant. The low amoxicillin concentration was also shifted into that quadrant, while the high AMX concentration returned the hemin community to the zero-iron AMX-treated group.

We next examined the OD-normalized relative abundance of the communities and observed shifts in four major genera in response to the combined effects of increased hemin and amoxicillin: *Bacteroides, Escherichia-Shigella, Parabacteroides,* and *Parasutterella*, shown in bold in the Legend (Figure 3D). The significance of these changes was confirmed through MaAsLin2, and independently graphed and shown in Figure 3E-G & Figure S1A. The *Bacteroides* genus, without additional hemin, initially bloom in low amoxicillin but are

eventually reduced at higher amoxicillin concentrations. The addition of + 15 μM hemin changes this dynamic, stabilizing the relative abundance numbers for the group when treated with antibiotics. When given + 60 μM hemin, *Bacteroides* are further stabilized, and even bloom with AMX (Figure 3D-E). We tested the MIC of two representative species of this genus, *B fragilis* and *B thetaiotaomicron*. The addition of increasing amounts of hemin to culture media did not significantly shift the MIC_{90} of either of these species (Figure S1C-D). It should be noted that the *Bacteroides* genus shifting in Figure 3D is comprised almost exclusively of an undetermined species of *Bacteroides*, and this phenomenon originally observed may be unique to this species.

In the presence of amoxicillin, *Escherichia-Shigella* does not expand until supplemented with + 60 μM hemin, allowing for a shift in overall resistance to amoxicillin and allowing for major growth in 2 μg/mL of amoxicillin. High hemin concentrations also support a large bloom in normalized relative abundance of *Escherichia-Shigella* without the presence of AMX (Figure 3D, 3F). We also found with *E. coli* Nissle 1917 that hemin supplementation increased the MIC_{90} at least 10-fold (Figure S1E). It should be noted that this strain of *E. coli* is not the same strain seen in our dataset. *Parabacteroides* and *Parasutterella* both exhibited a bloom in the presence of amoxicillin and high hemin concentrations in the media (Figure 3G, Figure S1A). indicating that the hemin may be having a protective effect against these genera against amoxicillin susceptibility.

The genus Enterococcus showed no significant change to amoxicillin susceptibility in response to increasing amoxicillin but did show interesting nonsignificant trends, leading us to the impact of hemin on the MIC_{90} of an *E. faecalis* strain. We found that giving this strain hemin at any concentrations lead to a drastic drop in the MIC_{90} to about 1/10 of control conditions

(Figure S1B, S1F). indicating that hemin drastically sensitized this strain of *E. faecalis* to antibiotic killing.

3.4 Free, Soluble Iron Provides Minimal Impact on Microbial Community Makeup

Iron can exist in many forms, both trapped in molecules like hemin, or in soluble forms in both ferric and ferrous iron. To test whether the phenomena identified with hemin was conserved amongst iron species or unique compared to free iron sources, the communities were grown and monitored for 24 hours in the presence of either $Fe(II)SO_4$ or $Fe(III)Cl_3$. The presence of free iron, either ferrous (II) or ferric (III), did not affect overall optical density of the cultures (Figure 4A). This holds true between amoxicillin treated groups, where it is shown that amoxicillin causes a stepwise reduction in OD_{600} but this drop is not influenced by the presence of free iron. The 24 hour cultures showed a drop in Shannon diversity in response to amoxicillin treatment in control iron groups, and this trend does not change between introduction of different sources and concentrations of iron, except the introduction of + 75 μM $FeCl_3$, which causes a reduction in the base Shannon diversity compared to the control iron group without amoxicillin, and a significant drop (# $p < 0.05$) in diversity when 2 μg/mL amoxicillin is added (Figure 4B). The Bray-Curtis dissimilarity PCoA plot showed that samples clustered by presence or absence of amoxicillin on the PC1 axis, and no difference in clustering between iron concentrations or groups (Figure 4C). The normalized relative abundance breakdown of the treated communities can be seen in Figure 4D, with the *Bacteroides, Escherichia-Shigella, Enterococcus,* and *Parabacteroides* genera shown separately (Figure 4E-F, Figure S2A-B).

Looking at the OD normalized relative abundance we found that in the absence of added free iron, *Bacteroides* was elevated by 2 μg/mL AMX but was fully eliminated at 10 μg/mL AMX. Iron supplementation in both free forms led to an elimination of *Bacteroides* at the protected low AMX concertation. This is a direct contradiction to the protection we observed with hemin, where further increases in hemin lead to increased amoxicillin protection. Percent growth curves generated for *B. fragilis* and *B. thetaiotaomicron* show that there is no change in MIC_{90} values for either species when grown in different concentrations and types of free iron (Figure S2C-D), indicating that iron in these strains does not increase amoxicillin susceptibility in the presence of different free iron sources. It should again be noted that the species identified within these samples contains mostly an unidentified species, and the unique effect hemin has as well as the lack of protection for free iron may be specific to this strain.

Similarly, *Escherichia-Shigella* did not show the same level of protection with free iron (Figure 4D, F) as with hemin (Figure 3D, F). We did observe that a higher concentration of $FeCl_3$ limits the growth of *Escherichia-Shigella* when grown without amoxicillin (Figure 4F), though amoxicillin susceptibility did not significantly change as a result of different forms of iron. The MIC_{90} of *E. coli* Nissle however does not change when given any type or concentration of iron (Figure S2E). This contradicts what was seen with hemin, where additions of hemin increased the MIC_{90} at least 10-fold. This indicates that *E. coli* is particularly adapted to using hemin to resist amoxicillin killing and not matching concentrations of free ferric or ferrous iron.

Parabacteroides do not grow well with the addition of any free form of iron, regardless of amoxicillin introduction (Figure S2A), which is contrary to the result seen with hemin in Figure 3D & Figure S3G where the bacteria was protected by supplementation and bloomed with hemin. The *Enterococcus* genus was also isolated and monitored. The addition of amoxicillin in

media with no iron supplementation cause a stepwise reduction of *Enterococcus* (Figure S2B). The genus also experienced a slight bloom in response to a small amount of amoxicillin when given $FeSO_4$ but not when given $FeCl_3$ and experienced a drop afterwards with large amounts of amoxicillin. The MIC_{90} for *E. faecalis* showed no changes in response to the introduction of different iron supplementations (Figure S2F). This contradicts the results seen in Figure S1F, where supplementation of hemin immediately potentiated the susceptibility of amoxicillin. This strain is not the dominant strain or species identified in our dataset and it should be noted that this may unique to *E. faecalis* UWH 1921.

Chapter 4: Discussion & Conclusion

4.1 Discussion

In this study, we aimed to (1) create a pipeline that uses *ex vivo* culturing techniques to allow for the study of the relationship between antibiotics and metabolic modulators on complex microbial makeup, and (2) deploy this pipeline to understand the relationship between different form of iron and amoxicillin susceptibility on complex microbial communities. The role metabolism has on antibiotic susceptibility has not been fully explored. Approximately 25% of individuals worldwide suffer from some form of anemia, with a majority of cases caused from iron deficiency,[104] so studying the effect antibiotics have on individuals requiring iron supplementation is important for global human health. This pipeline, in its current state, can successfully discern between bacteria at the species level in both synthetic communities and unknown complex microbial communities derived from murine and human samples. A dual barcoding approach allows for the multiplexing of 2304 samples generated from a single community input to be placed onto a single chip, drastically reducing the per sample cost in generation of data. This pipeline may be used to test the effects of other metabolic modifiers, such as carbon source. The culturing portion of the pipeline also allows for real-time monitoring of community growth, which cannot be conventionally performed in murine models. The implementation of a DNA cleanup step was also shown to be successful in removal of dead bacteria's DNA that otherwise would be represented in the data and confound results. The generation of frozen stool cultures derived from stool samples cultured to exponential growth phase allows for us to generate substantially more data from a single stool sample as each frozen stool culture aliquot can generate large numbers of consistent individual cultures for treating and sequencing. The culturing of human stool samples showed that the *ex vivo* culturing does not

alter the alpha or beta diversity of the community over 48 hours. These cultures are also relatively stable, and can support 78% of species over 24 hours, validating this particular pipeline as an alternative method for gaining preliminary data on combinational effects between antibiotics and metabolic modulators. As culture times increase, however, the power of this approach to retain species diminishes, and reducing culturing times should be taken into consideration.

Treatment of microbial communities with amoxicillin mirrored results seen *in vivo*, where introduction of antibiotics caused a bloom of *Bacteroidetes* and *Proteobacteria.*[76, 78, 98] These blooms can likely be attributed to a combination of intrinsic resistances and metabolically induced tolerance. When cultures were treated with various forms of iron, hemin was shown to have the most drastic effect on the communities' growth and community makeup when combined with amoxicillin. Treatment of communities that were co-supplemented with hemin with higher amounts of amoxicillin displayed increased overall growth that rivaled OD_{600} values of untreated, unsupplemented cultures after 24 hours. These communities were dominated by four particular genera when treated with a combination of hemin and amoxicillin: *Bacteroides, Escherichia-Shigella, Parabacteroides,* and *Parasutterella*. These genera were protected against amoxicillin killing in the presence of hemin. The increase in *Bacteroides* and *Parabacteroides* due to iron and antibiotic combination effects has been previously reported in murine models, though this increase was reported due to the addition of iron (II) sulfate to murine diets, rather than hemin.[98]

Bacteroides are abundant in the gut microbiome,[105-107] meaning that major alterations in abundances can lead to dysbiosis and issues to health; they can also act as opportunistic pathogens and have been isolated from infections across the body.[105, 106, 108] *Bacteroides* are

capable of sequestering iron and harnessing the use of siderophores produced by not only themselves, but other bacteria, in order to obtain iron.[109, 110] In particular, *B. vulgatus* can avoid spending energy on iron retrieval resources through using siderophores produced from other species.[111] *B. vulgatus* also has been shown to employ a specific ferrous iron transporter FeoAB to resist metronidazole through the import of iron molecules.[112] Heme molecules have been shown to further support the growth of *B. thetaiotaomicron*, though this had no effect on overall MIC_{90} values in our data *in vitro*.[113] The *Parasutterella* genus blooms in the presence of higher concentrations of amoxicillin when the media is supplemented with higher concentrations of hemin. *Parasutterella* are considered key members of the GI tract microbiome in humans,[114] and major increases in *Parasutterella* levels have been implicated in various disease states such as Crohn's Disease and obesity.[115-117] In previously reported data, the genus *Parasutterella* and *P. excrementihominis* both increase in high iron environments when treated with amoxicillin, though this is due to free iron.[98] The genus *Parabacteroides* also blooms in the presence of amoxicillin when supplemented with high concentrations of hemin. The *Parabacteroides* genus is also a major component of the healthy gut microbiome,[118] much like Bacteroides. The *Escherichia-Shigella* genus also exhibited a shift in antibiotic susceptibility with increasing hemin concentrations and shifted the elimination of *Escherichia-Shigella* from less than 2 μg/mL to greater than 2μg/mL *in vivo*, and increased the MIC_{90} of *E. coli* 10-fold *in vitro*. The addition of much higher concentrations of $FeCl_3$, however, has been shown to have no effect on the MLC of *E. coli*,[119] hinting that this effect is unique to hemin. While some *E. coli* and *Shigella* strains are key food-borne pathogens, others tend to be relatively harmless or beneficial to the microbiome's homeostasis.[120-122] Some studies have shown that high iron supports the growth of *E. coli in vitro* and *in vivo*.[123, 124] Other studies used iron chelators aerobically to show that

reductions in iron reduced ampicillin killing, another antibiotic of the penicillin class.[91] The difference in observed results may be explained by different forms of iron used or that our work was performed anaerobically where the production of hydroxyl radicals from the Fenton reaction is less applicable.

Free iron supplementation into the media on the other hand did not seem to have as drastic on effect on antibiotic susceptibility as a whole. Overall, the change in optical density over time was not affected by the presence of any type or concentration of iron that was matched in concentration to that of hemin previously mentioned. Free iron also did not significantly alter the diversity of these samples. The presence of 75 μM $FeCl_3$ prevented growth of *Bacteroides*, *Escherichia-Shigella*, *Parabacteroides*, and *Parasutterella*. The phenomenon we observed with high concentrations of hemin on antibiotic susceptibility was not present when treated with free ferric iron. It should be noted that, though murine models have shown increases in *Bacteroides* and *Parasutterella* when given free iron and antibiotics, these mice are given substantially higher concentrations of dietary $FeSO_4$ (500mg/kg) and are subject to oral metronidazole and neomycin treatment rather than amoxicillin.[98] The genus *Clostridium sensu stricto 1*, however, does experience an increase in antibiotic resistance to amoxicillin as a result to supplementation of the media with free Fe (III). This genus contains a large number of both pathogens like *C. botulinum and C. tetani*, as well as beneficial species such as *C. butyricum*.[125-128] Some strains of *C. butyricum* have been identified as pathogenic, however, through their ability to produce toxins like botulinum neurotoxin.[129] It is likely that the taxa identified as *Clostridium senso stricto 1* in our dataset is *C. butyricum*. The genus *Bifidobacterium* also grows in the presence of free Fe (II) and further increases of iron sulfate allow for a shift in amoxicillin susceptibility; *Bifidobacterium* blooms in the presence of 2 μg/mL amoxicillin when treated with 75 μM $FeSO_4$.

Many *Bifidobacterium* species have the capacity to retain iron due to sufficient iron sequestration mechanisms.[130, 131] In our dataset, these species were identified as *B. longum, B. kashiwanohense, B. adolescentis,*and *B. breve*. Overall, with the exception of 75 μM $FeCl_3$, we saw quite similar results with free ferric and ferrous iron, likely explained through the reduction of Fe^{3+} to Fe^{2+} anaerobically.[132]

The bacteria that were protected against amoxicillin killing through the supplementation of hemin are all robust regulators of iron entering and exiting the cell; thus, they are much more likely to maintain iron at optimal levels with and without supplementation. However, during supplementation they are uniquely able to use a variety of techniques for sequestering iron from their environment. Siderophores produced by these bacteria are also much more efficient at removing iron from cofactors such as hemin than obtaining free iron.[133-135] *E. coli* strains have been shown to produce a variety of iron uptake systems, and more virulent strains are shown to produce more siderophores.[136, 137] The key question brought up by our work is why doesn't hemin induce susceptibility as expected based on the role of iron in elevated metabolism. The key aspect is the anaerobic nature of our experiment where the added toxicity of iron through oxidative damage may not play a role in antimicrobial potentiation. In fact, a higher abundance of iron may support lower levels of metabolic activity required for damage and stress responses. An additional explanation is that the surviving species may have intrinsic beta-lactam resistance mechanisms that are either supported by or exaggerated by iron supplementation. In other words, if a microbe can survive amoxicillin, additional iron supplementation may allow it to outcompete other members of the community. It is also plausible that these cells are allocating resources towards iron regulation and uptake that may otherwise be used in futile cycling processes that would potentiate antibiotic susceptibility. In order to identify if this is the case,

metatranscriptomics could be performed to identify whether or not this is the case for these particular genera. In this analysis, it would be important to look for markers of antimicrobial response such as the SOS response or other general stress responses[77, 138, 139] in combination with signatures of metabolic activity.[77] For example, if iron availability upregulates metabolism while amoxicillin does not elicit a stress response, this would indicate that iron-based protection is acting through a resistance-growth enhancement direction. On the other hand, if iron availability reduces metabolic activity while the antibiotics do indeed trigger a stress response, this would indicate that iron leads to reduction through reduction of metabolic activity. Finally, it is also possible that both metabolism and the stress responses are upregulated at the same time, likely indicating a protection mediated by an elevated capacity to deal with cellular damage.

4.2 Conclusion

The global rise of antibiotic-resistant infections underscores the urgent need for new strategies to enhance antibiotic efficacy, particularly within complex microbial ecosystems like the human gut. Such strategies can be developed and systematically tested using *ex vivo* systems that preserve the structure and diversity of native microbial communities while enabling controlled, high-throughput experimentation. The use of iron to potentiate amoxicillin susceptibility has promise as a combinational therapeutic approach to eliminate bacteria naturally resistant to amoxicillin. In this study, we employed a unique *ex vivo* culturing approach to monitor the effects of iron on antibiotic susceptibility. This pipeline allows for a high level of consistency in community inputs for an apples-to-apples comparison in susceptibility. This study showed that, contrary to expectation, higher concentrations of ferric iron trapped in a cofactor (hemin) caused communities to bloom when they were treated with amoxicillin. These

communities were dominated by genera in the phyla Bacteroidetes and Proteobacteria: *Bacteroides*, *Escherichia-Shigella*, *Parabacteroides*, and *Parasutterella*. This protection was not seen, however, when matched concentrations of free iron were added to the communities and treated with amoxicillin. These findings suggest that the form of iron—not just its presence—can critically shape microbial community resilience under antibiotic stress, likely through modulation of species-specific metabolic pathways and stress responses.

Given the widespread use of both antibiotics and iron supplements, especially in vulnerable populations such as those with iron-deficiency anemia, these results have important clinical implications. Understanding how metabolic context influences antibiotic efficacy may help optimize therapeutic regimens and minimize off-target impacts on the microbiome.

Furthermore, our *ex vivo* pipeline offers a powerful platform to test a wide range of metabolic or dietary interventions in combination with antimicrobials. Future work employing transcriptomics, metabolomics, and ultimately *in vivo* validation will be essential to uncover the mechanisms underlying hemin-mediated protection and determine whether these effects can be harnessed—or mitigated—to improve clinical outcomes.

While this study demonstrates the utility of *ex vivo* systems in profiling metabolic modulation of antibiotic susceptibility, several limitations should be noted. Host factors are absent in this model, and media composition may bias community growth. Although community structure was largely preserved in the short time frame, extended culturing reduced species retention. Only one human-derived microbiome was tested, which enabled experimental consistency but limited generalizability across diverse hosts. Some taxa remained unclassified at the species level, and antibiotic susceptibility was validated only for selected isolates. Lastly, the

protective effects of hemin remain mechanistically unresolved and require functional validation through transcriptomics or metabolomics.

Figure Legends

Figure 1: Establishment of pipeline in synthetic consortia community & murine cecal communities. (A) Experimental design for culturing various community inputs to obtain sequencing data. Figure was created using Biorender. (B) Average relative abundances of species comprising a synthetic community treated with or without amoxicillin over 24 hours. Data are represented as average relative abundance for n = 3 to 5 replicates. (C) Average relative abundance of species of the synthetic community spiked with *E. coli* killed from 100 μg/mL AMX and treated with DNA Cleanup step. Data are represented as average relative abundance ± STD for n = 4. (D) Average normalized relative abundances of families within cecal communities treated with or without amoxicillin and/or the DNA cleanup step for 24 hours. Families in bold represent families that are reduced in response to the cleanup step, while families underlined increase in response to the cleanup step. Data are represented as average relative abundance normalized against the highest OD_{600} ± STD for n = 6.

Figure 2: Validation of community culturing pipeline shows successful species retention over a 48-hour period. (A) Alpha diversity of clinical patient derived human stool sample cultures as measured by Shannon diversity index. Black lines in the box & whisker plot indicate the mean, with whiskers identifying minimum and maximums of the data for n = 1-16. (B) PCoA of beta diversity of samples via Bray-Curtis Dissimilarity. (C) Average relative abundance of bacteria families of culture samples over 48 hours. Data are represented as average relative abundance ± STD for n = 1-8. (D) Percent species still present after culturing samples over 24 and 48 hours. Data are represented as the number of species that retain at least 1% of their input community's makeup divided by the total number of species identified in the community makeup and presented as an average percent.

Figure 3: Hemin supplementation in media provides protection against amoxicillin susceptibility for four genera in human microbial sample cultures. (A) Optical density at 600 nm of microbial human stool sample cultures measured every 30 minutes over 24 hours. Data are represented as means of OD_{600} of n = 6. (B). Alpha diversity of sample cultures as measured by Shannon diversity index. Black lines indicate the mean, with whiskers identifying minimum and maximums of the data for n = 4. (* $p < 0.05$, compared to 0 μg/mL AMX in + 0 μM hemin concentration; # $p < 0.05$, compared to 0 μg/mL AMX in same hemin conditions). (C) PCoA of beta diversity of samples via Bray-Curtis Dissimilarity. (D). Average normalized relative abundances of genera. Top 23 genera are shown, with all other genera consolidated to "Other". Genera in bold showed significance through MaAsLin2 due to the combinational effects of hemin and amoxicillin (FDR > 0.05). Data are represented as average relative abundance normalized against highest OD_{600} of experiment ± STD for n = 4. (E) Average normalized relative abundance of *Bacteroides* genus extrapolated from Figure 3D. Data are represented as average relative abundance normalized against highest OD_{600} of experiment ± STD for n = 4. (F) Average normalized relative abundance of *Escherichia-Shigella* genus extrapolated from Figure 3D. Data are represented as average relative abundance normalized against highest OD_{600} of experiment ± STD for n = 4. (G) Average normalized relative abundance of *Parabacteroides* genus extrapolated from Figure 3D. Data are represented as average relative abundance normalized against highest OD_{600} of experiment ± STD for n = 4.

Figure 4: Free ferric and ferrous iron minimally impacts human microbial sample community makeup. (A) Optical density at 600 nm of microbial human stool sample cultures measured every 30 minutes over 24 hours. Data are represented as means of OD_{600} of n = 6. (B). Alpha diversity of sample cultures as measured by Shannon diversity index. Black lines indicate

the mean, with whiskers identifying minimum and maximums of the data for n = 4. (* $p < 0.05$, compared to 0 μg/mL AMX in + 0 μM free iron concentration; # $p < 0.05$, compared to 0 μg/mL AMX in same free iron conditions). (C) PCoA of beta diversity of samples via Bray-Curtis Dissimilarity. (D). Average normalized relative abundances of genera. Top 15 genera are shown, with all other genera consolidated to "Other". Genera in bold showed reduction to abundances in response to amoxicillin when given free iron. Data are represented as average relative abundance normalized against highest OD_{600} of experiment ± STD for n = 4. (E) Average normalized relative abundance of *Bacteroides* genus extrapolated from Figure 4D. Data are represented as average relative abundance normalized against highest OD_{600} of experiment ± STD for n = 4. (F) Average normalized relative abundance of *Escherichia-Shigella* genus extrapolated from Figure 4D. Data are represented as average relative abundance normalized against highest OD_{600} of experiment ± STD for n = 4.

Figures

Figure 1: Establishment of pipeline in synthetic consortia community & murine cecal communities.

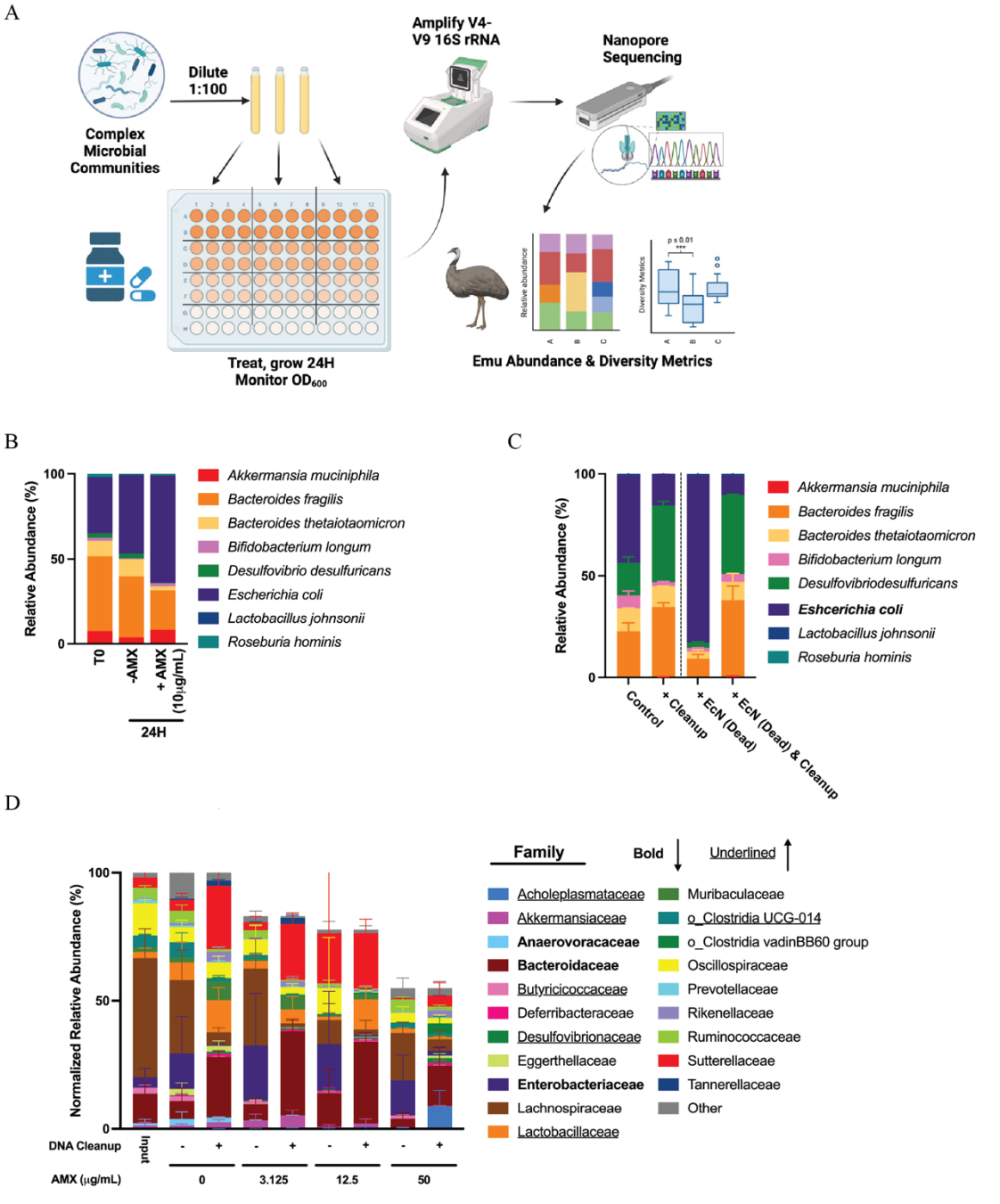

Figure 2: Validation of community culturing pipeline shows successful species retention over a 48 hour period.

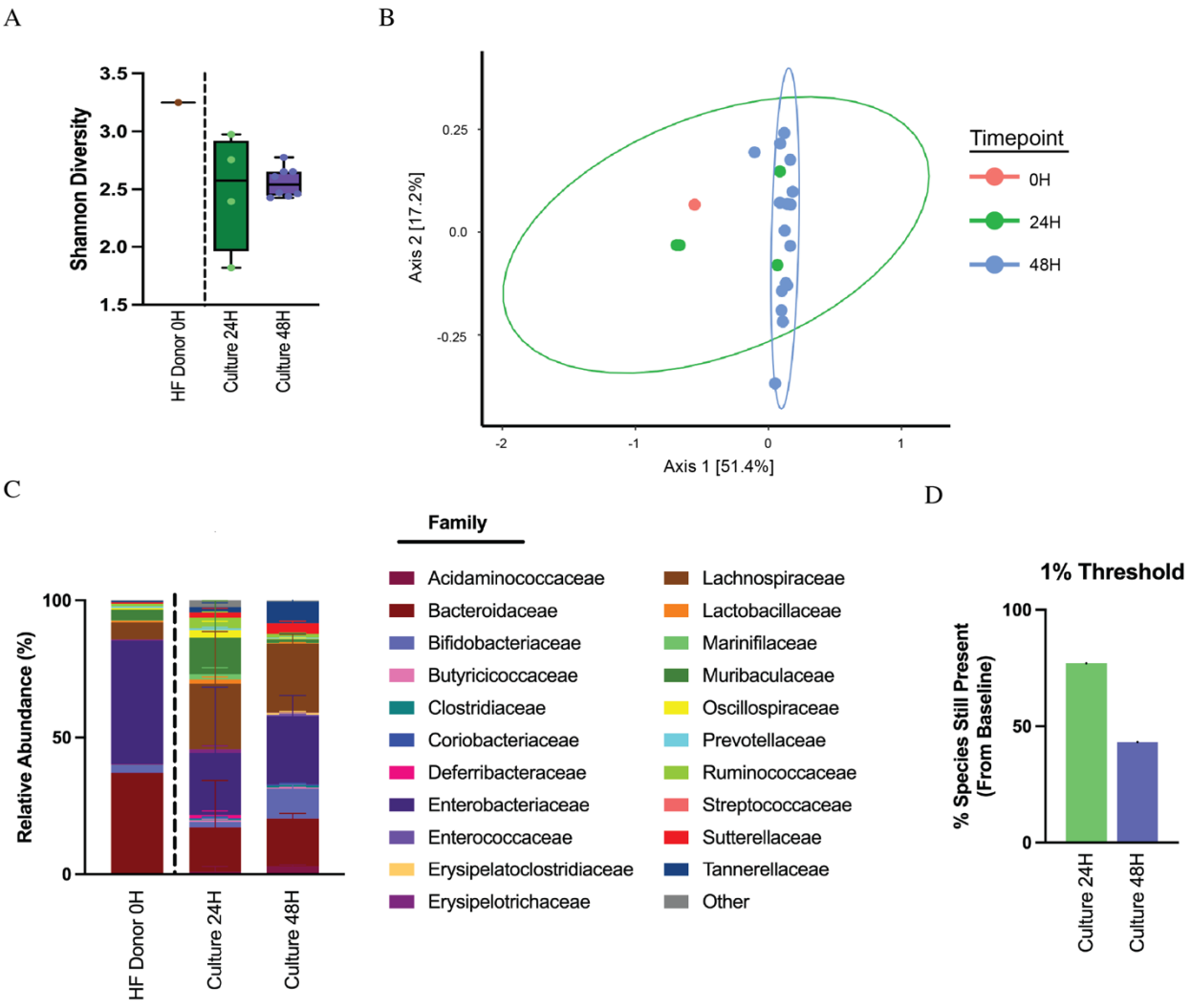

Figure 3: Hemin supplementation in media provides protection against amoxicillin susceptibility for four genera in human microbial sample cultures.

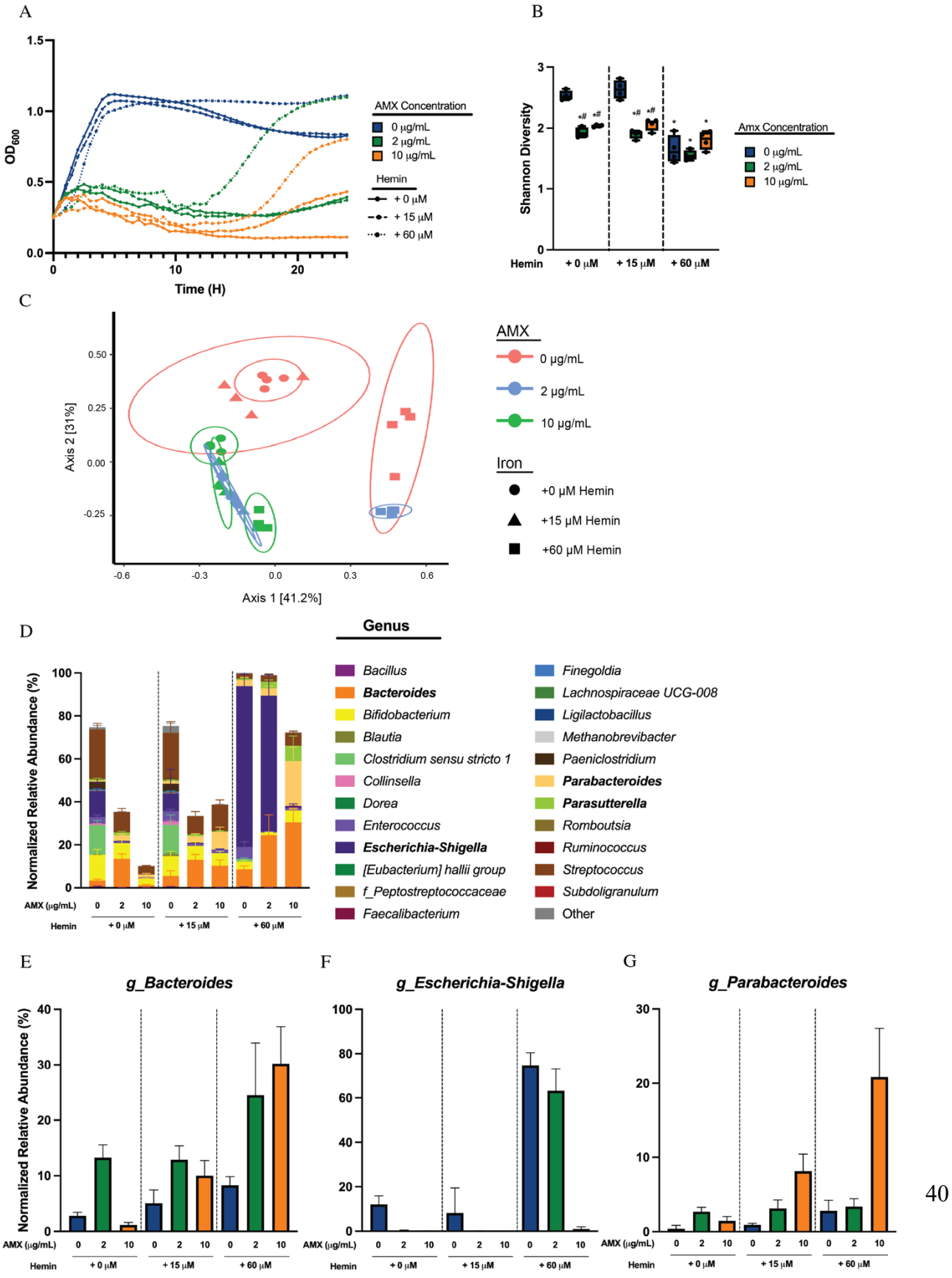

Figure 4: Free ferric and ferrous iron minimally impacts human microbial sample community makeup.

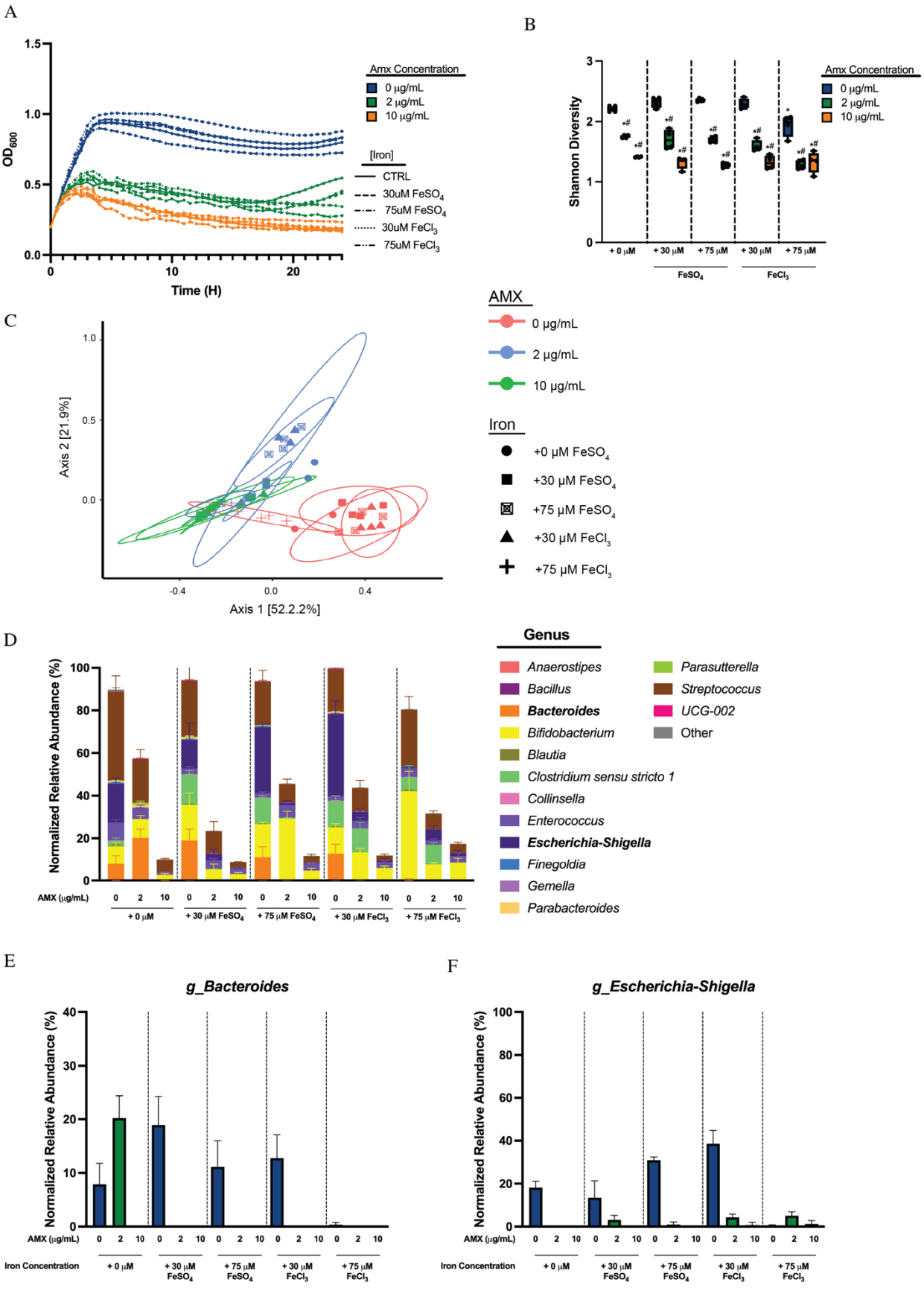

Tables

Table 1: List of Bacteria Species Used to Generate Data

Species	**Strain**	**Origin**	**Origin #**	**Phylum**
Akkermansia muciniphila		DSMZ		Verrucomicrobiota
Bacteroides fragilis	VPI 2553	ATCC	ATCC 25285	Bacteroidetes
Bacteroides thetaiotaomicron	VPI 5482	ATCC	ATCC 29148	Bacteroidetes
Bifidobacterium longum	E194b	DSMZ	DSM 20219	Actinobacteria
Desulfovibrio desulfuricans	Essex Type 6	DSMZ	DSM 642	Proteobacteria
Enterococcus faecalis	UWH 1921	ATCC	ATCC 49532	Firmicutes
Escherichia coli	Nissle 1917	Ardeypharm		Proteobacteria
Lactobacillus johnsonii	VPI 7960	DSMZ	DSM 10533	Firmicutes
Roseburia hominis	A2-183	DSMZ	DSM 16839	Firmicutes

Table 2: List of Reverse Primers Used for Multiplexing

Name	**Barcode**	**Link**	**1492R Primer**	**Full Sequence**
Rev_BC01	AGCCTTCGTCGC	CC	CGGCTACCTTGTTAC GAC	AGCCTTCGTCGCCCCG GCTACCTTGTTACGAC
Rev_BC02	TCCATACCGGAA	CC	CGGCTACCTTGTTAC GAC	TCCATACCGGAACCCG GCTACCTTGTTACGAC
Rev_BC03	AGCCCTGCTACA	CC	CGGCTACCTTGTTAC GAC	AGCCCTGCTACACCCG GCTACCTTGTTACGAC
Rev_BC04	CCTAACGGTCCA	CC	CGGCTACCTTGTTAC GAC	CCTAACGGTCCACCCG GCTACCTTGTTACGAC
Rev_BC05	CGCGCCTTAAAC	CC	CGGCTACCTTGTTAC GAC	CGCGCCTTAAACCCCG GCTACCTTGTTACGAC
Rev_BC06	TATGGTACCCAG	CC	CGGCTACCTTGTTAC GAC	TATGGTACCCAGCCCG GCTACCTTGTTACGAC
Rev_BC07	TACAATATCTGT	CC	CGGCTACCTTGTTAC GAC	TACAATATCTGTCCCG GCTACCTTGTTACGAC
Rev_BC08	AATTTAGGTAGG	CC	CGGCTACCTTGTTAC GAC	AATTTAGGTAGGCCCG GCTACCTTGTTACGAC

Rev_BC09	GACTCAACCAGT	CC	CGGCTACCTTGTTAC GAC	GACTCAACCAGTCCCG GCTACCTTGTTACGAC
Rev_BC10	GCCTCTACGTCG	CC	CGGCTACCTTGTTAC GAC	GCCTCTACGTCGCCCG GCTACCTTGTTACGAC
Rev_BC11	ACTACTGAGGAT	CC	CGGCTACCTTGTTAC GAC	ACTACTGAGGATCCCG GCTACCTTGTTACGAC
Rev_BC12	AATTCACCTCCT	CC	CGGCTACCTTGTTAC GAC	AATTCACCTCCTCCCG GCTACCTTGTTACGAC
Rev_BC13	CGTATAAATGCG	CC	CGGCTACCTTGTTAC GAC	CGTATAAATGCGCCCG GCTACCTTGTTACGAC
Rev_BC14	ATGCTGCAACAC	CC	CGGCTACCTTGTTAC GAC	ATGCTGCAACACCCCG GCTACCTTGTTACGAC
Rev_BC15	ACTCGCTCGCTG	CC	CGGCTACCTTGTTAC GAC	ACTCGCTCGCTGCCCG GCTACCTTGTTACGAC
Rev_BC16	TTCCTTAGTAGT	CC	CGGCTACCTTGTTAC GAC	TTCCTTAGTAGTCCCG GCTACCTTGTTACGAC
Rev_BC17	CGTCCGTATGAA	CC	CGGCTACCTTGTTAC GAC	CGTCCGTATGAACCCG GCTACCTTGTTACGAC

Rev_BC18	ACGTGAGGAACG	CC	CGGCTACCTTGTTAC GAC	ACGTGAGGAACGCCC GGCTACCTTGTTACGA C
Rev_BC19	GGTTGCCCTGTA	CC	CGGCTACCTTGTTAC GAC	GGTTGCCCTGTACCCG GCTACCTTGTTACGAC
Rev_BC20	CATATAGCCCGA	CC	CGGCTACCTTGTTAC GAC	CATATAGCCCGACCCG GCTACCTTGTTACGAC
Rev_BC21	GCCTATGAGATC	CC	CGGCTACCTTGTTAC GAC	GCCTATGAGATCCCCG GCTACCTTGTTACGAC
Rev_BC22	CAAGTGAAGGG A	CC	CGGCTACCTTGTTAC GAC	CAAGTGAAGGGACCC GGCTACCTTGTTACGA C
Rev_BC23	CACGTTTATTCC	CC	CGGCTACCTTGTTAC GAC	CACGTTTATTCCCCCG GCTACCTTGTTACGAC
Rev_BC24	TAATCGGTGCCA	CC	CGGCTACCTTGTTAC GAC	TAATCGGTGCCACCCG GCTACCTTGTTACGAC
Rev_BC25	TGACTAATGGCC	CC	CGGCTACCTTGTTAC GAC	TGACTAATGGCCCCCG GCTACCTTGTTACGAC

Rev_BC26	CGGGACACCCGA	CC	CGGCTACCTTGTTAC GAC	CGGGACACCCGACCC GGCTACCTTGTTACGA C
Rev_BC27	CTGTCTATACTA	CC	CGGCTACCTTGTTAC GAC	CTGTCTATACTACCCG GCTACCTTGTTACGAC
Rev_BC28	TATGCCAGAGAT	CC	CGGCTACCTTGTTAC GAC	TATGCCAGAGATCCCG GCTACCTTGTTACGAC
Rev_BC29	CGTTTGGAATGA	CC	CGGCTACCTTGTTAC GAC	CGTTTGGAATGACCCG GCTACCTTGTTACGAC
Rev_BC30	AAGAACTCATGA	CC	CGGCTACCTTGTTAC GAC	AAGAACTCATGACCC GGCTACCTTGTTACGA C
Rev_BC31	TGATATCGTCTT	CC	CGGCTACCTTGTTAC GAC	TGATATCGTCTTCCCG GCTACCTTGTTACGAC
Rev_BC32	CGGTGACCTACT	CC	CGGCTACCTTGTTAC GAC	CGGTGACCTACTCCCG GCTACCTTGTTACGAC
Rev_BC33	AATGCGCGTATA	CC	CGGCTACCTTGTTAC GAC	AATGCGCGTATACCCG GCTACCTTGTTACGAC
Rev_BC34	CTTGATTCTTGA	CC	CGGCTACCTTGTTAC GAC	CTTGATTCTTGACCCG GCTACCTTGTTACGAC

Rev_BC35	GAAATCTTGAAG	CC	CGGCTACCTTGTTAC GAC	GAAATCTTGAAGCCC GGCTACCTTGTTACGA C
Rev_BC36	GAGATACAGTTC	CC	CGGCTACCTTGTTAC GAC	GAGATACAGTTCCCCG GCTACCTTGTTACGAC
Rev_BC37	GTGGAGTCTCAT	CC	CGGCTACCTTGTTAC GAC	GTGGAGTCTCATCCCG GCTACCTTGTTACGAC
Rev_BC38	ACCTTACACCTT	CC	CGGCTACCTTGTTAC GAC	ACCTTACACCTTCCCG GCTACCTTGTTACGAC
Rev_BC39	TAATCTCGCCGG	CC	CGGCTACCTTGTTAC GAC	TAATCTCGCCGGCCCG GCTACCTTGTTACGAC
Rev_BC40	ATCTAGTGGCAA	CC	CGGCTACCTTGTTAC GAC	ATCTAGTGGCAACCCG GCTACCTTGTTACGAC
Rev_BC41	ACGCTTAACGAC	CC	CGGCTACCTTGTTAC GAC	ACGCTTAACGACCCCG GCTACCTTGTTACGAC
Rev_BC42	TACGGATTATGG	CC	CGGCTACCTTGTTAC GAC	TACGGATTATGGCCCG GCTACCTTGTTACGAC
Rev_BC43	ATACATGCAAGA	CC	CGGCTACCTTGTTAC GAC	ATACATGCAAGACCC GGCTACCTTGTTACGA C

Rev_BC44	CTTAGTGCAGAA	CC	CGGCTACCTTGTTAC GAC	CTTAGTGCAGAACCCG GCTACCTTGTTACGAC
Rev_BC45	AATCTTGCGCCG	CC	CGGCTACCTTGTTAC GAC	AATCTTGCGCCGCCCG GCTACCTTGTTACGAC
Rev_BC46	AGGATCAGGGA A	CC	CGGCTACCTTGTTAC GAC	AGGATCAGGGAACCC GGCTACCTTGTTACGA C
Rev_BC47	AATAACTAGGGT	CC	CGGCTACCTTGTTAC GAC	AATAACTAGGGTCCC GGCTACCTTGTTACGA C
Rev_BC48	TATTGCAGCAGC	CC	CGGCTACCTTGTTAC GAC	TATTGCAGCAGCCCCG GCTACCTTGTTACGAC
Rev_BC49	TGATGTGCTAAG	CC	CGGCTACCTTGTTAC GAC	TGATGTGCTAAGCCCG GCTACCTTGTTACGAC
Rev_BC50	GTAGTAGACCAT	CC	CGGCTACCTTGTTAC GAC	GTAGTAGACCATCCCG GCTACCTTGTTACGAC
Rev_BC51	AGTAAAGATCGT	CC	CGGCTACCTTGTTAC GAC	AGTAAAGATCGTCCC GGCTACCTTGTTACGA C

Rev_BC52	CTCGCCCTCGCC	CC	CGGCTACCTTGTTAC GAC	CTCGCCCTCGCCCCCG GCTACCTTGTTACGAC
Rev_BC53	TCTCTTTCGACA	CC	CGGCTACCTTGTTAC GAC	TCTCTTTCGACACCCG GCTACCTTGTTACGAC
Rev_BC54	ACATACTGAGCA	CC	CGGCTACCTTGTTAC GAC	ACATACTGAGCACCC GGCTACCTTGTTACGA C
Rev_BC55	GTTGATACGATG	CC	CGGCTACCTTGTTAC GAC	GTTGATACGATGCCCG GCTACCTTGTTACGAC
Rev_BC56	GTCAACGCTGTC	CC	CGGCTACCTTGTTAC GAC	GTCAACGCTGTCCCCG GCTACCTTGTTACGAC
Rev_BC57	TGAGACCCTACA	CC	CGGCTACCTTGTTAC GAC	TGAGACCCTACACCCG GCTACCTTGTTACGAC
Rev_BC58	ACTTGGTGTAAG	CC	CGGCTACCTTGTTAC GAC	ACTTGGTGTAAGCCCG GCTACCTTGTTACGAC
Rev_BC59	ATTACGTATCAT	CC	CGGCTACCTTGTTAC GAC	ATTACGTATCATCCCG GCTACCTTGTTACGAC
Rev_BC60	CACGCAGTCTAC	CC	CGGCTACCTTGTTAC GAC	CACGCAGTCTACCCCG GCTACCTTGTTACGAC

Rev_BC61	TGTGCACGCCAT	CC	CGGCTACCTTGTTAC GAC	TGTGCACGCCATCCCG GCTACCTTGTTACGAC
Rev_BC62	CCGGACAAGAA G	CC	CGGCTACCTTGTTAC GAC	CCGGACAAGAAGCCC GGCTACCTTGTTACGA C
Rev_BC63	TTGCTGGACGCT	CC	CGGCTACCTTGTTAC GAC	TTGCTGGACGCTCCCG GCTACCTTGTTACGAC
Rev_BC64	TACTAACGCGGT	CC	CGGCTACCTTGTTAC GAC	TACTAACGCGGTCCCG GCTACCTTGTTACGAC
Rev_BC65	GCGATCACACCT	CC	CGGCTACCTTGTTAC GAC	GCGATCACACCTCCCG GCTACCTTGTTACGAC
Rev_BC66	CAAACGCACTAA	CC	CGGCTACCTTGTTAC GAC	CAAACGCACTAACCC GGCTACCTTGTTACGA C
Rev_BC67	GAAGAGGGTTGA	CC	CGGCTACCTTGTTAC GAC	GAAGAGGGTTGACCC GGCTACCTTGTTACGA C
Rev_BC68	TGAGTGGTCTGT	CC	CGGCTACCTTGTTAC GAC	TGAGTGGTCTGTCCCG GCTACCTTGTTACGAC

Rev_BC69	TTACACAAAGGC	CC	CGGCTACCTTGTTAC GAC	TTACACAAAGGCCCC GGCTACCTTGTTACGA C
Rev_BC70	ACGACGCATTTG	CC	CGGCTACCTTGTTAC GAC	ACGACGCATTTGCCCG GCTACCTTGTTACGAC
Rev_BC71	TATCCAAGCGCA	CC	CGGCTACCTTGTTAC GAC	TATCCAAGCGCACCCG GCTACCTTGTTACGAC
Rev_BC72	AGAGCCAAGAG C	CC	CGGCTACCTTGTTAC GAC	AGAGCCAAGAGCCCC GGCTACCTTGTTACGA C
Rev_BC73	GGTGAGCAAGCA	CC	CGGCTACCTTGTTAC GAC	GGTGAGCAAGCACCC GGCTACCTTGTTACGA C
Rev_BC74	TAAATATACCCT	CC	CGGCTACCTTGTTAC GAC	TAAATATACCCTCCCG GCTACCTTGTTACGAC
Rev_BC75	TTGCGGACCCTA	CC	CGGCTACCTTGTTAC GAC	TTGCGGACCCTACCCG GCTACCTTGTTACGAC
Rev_BC76	GTCGTCCAAATG	CC	CGGCTACCTTGTTAC GAC	GTCGTCCAAATGCCCG GCTACCTTGTTACGAC

Rev_BC77	TGCACAGTCGCT	CC	CGGCTACCTTGTTAC GAC	TGCACAGTCGCTCCCG GCTACCTTGTTACGAC
Rev_BC78	TTACTGTGGCCG	CC	CGGCTACCTTGTTAC GAC	TTACTGTGGCCGCCCG GCTACCTTGTTACGAC
Rev_BC79	GGTTCATGAACA	CC	CGGCTACCTTGTTAC GAC	GGTTCATGAACACCCG GCTACCTTGTTACGAC
Rev_BC80	TAACAATAATTC	CC	CGGCTACCTTGTTAC GAC	TAACAATAATTCCCCG GCTACCTTGTTACGAC
Rev_BC81	CTTATTAAACGT	CC	CGGCTACCTTGTTAC GAC	CTTATTAAACGTCCCG GCTACCTTGTTACGAC
Rev_BC82	GCTCGAAGATTC	CC	CGGCTACCTTGTTAC GAC	GCTCGAAGATTCCCCG GCTACCTTGTTACGAC
Rev_BC83	TATTTGATTGGT	CC	CGGCTACCTTGTTAC GAC	TATTTGATTGGTCCCG GCTACCTTGTTACGAC
Rev_BC84	TGTCAAAGTGAC	CC	CGGCTACCTTGTTAC GAC	TGTCAAAGTGACCCCG GCTACCTTGTTACGAC
Rev_BC85	CTATGTATTAGT	CC	CGGCTACCTTGTTAC GAC	CTATGTATTAGTCCCG GCTACCTTGTTACGAC
Rev_BC86	ACTCCCGTGTGA	CC	CGGCTACCTTGTTAC GAC	ACTCCCGTGTGACCCG GCTACCTTGTTACGAC

Rev_BC87	CGGTATAGCAAT	CC	CGGCTACCTTGTTAC GAC	CGGTATAGCAATCCCG GCTACCTTGTTACGAC
Rev_BC88	GACTCTGCTCAG	CC	CGGCTACCTTGTTAC GAC	GACTCTGCTCAGCCCG GCTACCTTGTTACGAC
Rev_BC89	GTCATGCTCCAG	CC	CGGCTACCTTGTTAC GAC	GTCATGCTCCAGCCCG GCTACCTTGTTACGAC
Rev_BC90	TACCGAAGGTAT	CC	CGGCTACCTTGTTAC GAC	TACCGAAGGTATCCCG GCTACCTTGTTACGAC
Rev_BC91	TGAGTATGAGTA	CC	CGGCTACCTTGTTAC GAC	TGAGTATGAGTACCCG GCTACCTTGTTACGAC
Rev_BC92	AATGGTTCAGCA	CC	CGGCTACCTTGTTAC GAC	AATGGTTCAGCACCCG GCTACCTTGTTACGAC
Rev_BC93	GAACCAGTACTC	CC	CGGCTACCTTGTTAC GAC	GAACCAGTACTCCCCG GCTACCTTGTTACGAC
Rev_BC94	CGCACCCATACA	CC	CGGCTACCTTGTTAC GAC	CGCACCCATACACCC GGCTACCTTGTTACGA C
Rev_BC95	GTGCCATAATCG	CC	CGGCTACCTTGTTAC GAC	GTGCCATAATCGCCCG GCTACCTTGTTACGAC

Rev_BC96	ACTCTTACTTAG	CC	CGGCTACCTTGTTAC GAC	ACTCTTACTTAGCCCG GCTACCTTGTTACGAC

Supplementary Figure Legends

Figure S1: Relationship between hemin and amoxicillin susceptibility in some genera and effect of hemin on amoxicillin MIC_{90} in key species. (A) Average normalized relative abundance of *Parasutterella* genus extrapolated from Figure 3D. Data are represented as average relative abundance normalized against highest OD_{600} of experiment ± STD for n = 4. (B) Average normalized relative abundance of *Enterococcus* genus extrapolated from Figure 3D. Data are represented as average relative abundance normalized against highest OD_{600} of experiment ± STD for n = 4. (C) Percent growth curve of *B. fragilis* treated with amoxicillin and hemin. MIC_{90} calculated using Gompertz equation for MIC determination where % growth = 10%. Data represented as average percent growth ± STD for n = 3-6. (D) Percent growth curve of *B. thetaiotaomicron* treated with amoxicillin and hemin. MIC_{90} calculated using Gompertz equation for MIC determination where % growth = 10%. Data represented as average percent growth ± STD for n = 3-6. (E) Percent growth curve of *E. coli Nissle* treated with amoxicillin and hemin. MIC_{90} calculated using Gompertz equation for MIC determination where % growth = 10%. Data represented as average percent growth ± STD for n = 3-6. (F) Percent growth curve of *E. faecalis* treated with amoxicillin and hemin. MIC_{90} calculated using Gompertz equation for MIC determination where % growth = 10%. Data represented as average percent growth ± STD for n = 3.

Figure S2: Relationship between free iron and amoxicillin susceptibility in some genera and effects of free iron on amoxicillin MIC_{90} in key species. (A) Average normalized relative abundance of *Parabacteroides* genus extrapolated from Figure 4D. Data are represented as average relative abundance normalized against highest OD_{600} of experiment ± STD for n = 4.

(B) Average normalized relative abundance of *Enterococcus* genus extrapolated from Figure 4D. Data are represented as average relative abundance normalized against highest OD_{600} of experiment ± STD for n = 4. (C) Percent growth curve of *B. fragilis* treated with amoxicillin and free iron. MIC_{90} calculated using Gompertz equation for MIC determination where % growth = 10%. Data represented as average percent growth ± STD for n = 3. (D) Percent growth curve of *B. thetaiotaomicron* treated with amoxicillin and free iron. MIC_{90} calculated using Gompertz equation for MIC determination where % growth = 10%. Data represented as average percent growth ± STD for n = 3. (E) Percent growth curve of *E. coli Nissle* treated with amoxicillin and free iron. MIC_{90} calculated using Gompertz equation for MIC determination where % growth = 10%. Data represented as average percent growth ± STD for n = 3. (F) Percent growth curve of *E. faecalis* treated with amoxicillin and free iron. MIC_{90} calculated using Gompertz equation for MIC determination where % growth = 10%. Data represented as average percent growth ± STD for n = 3.

Supplementary Figures

Figure S1: Relationship between hemin and amoxicillin susceptibility in some genera and effect of hemin on amoxicillin MIC_{90} in key species.

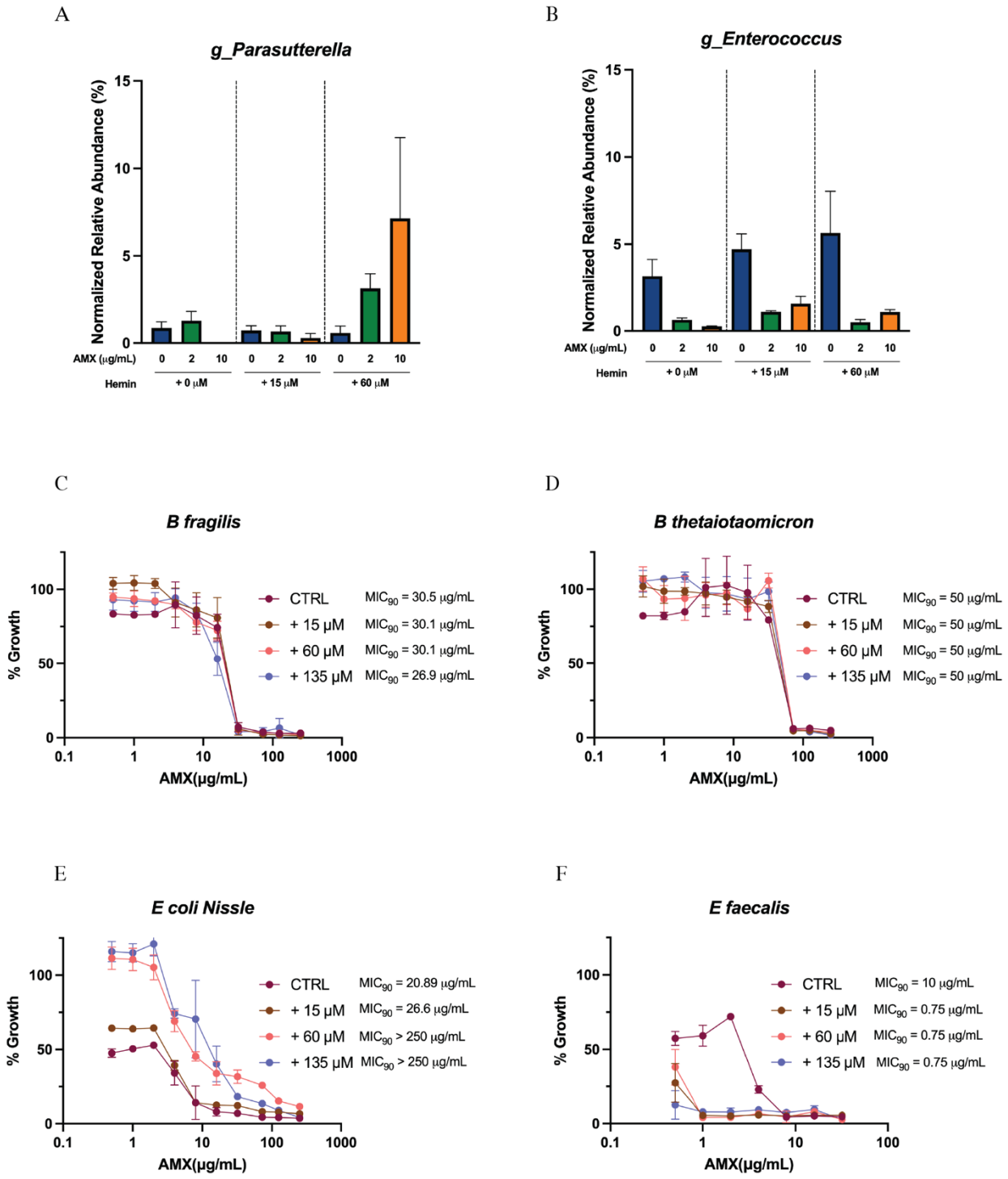

Figure S2: Relationship between free iron and amoxicillin susceptibility in some genera and effects of free iron on amoxicillin MIC_{90} in key species.

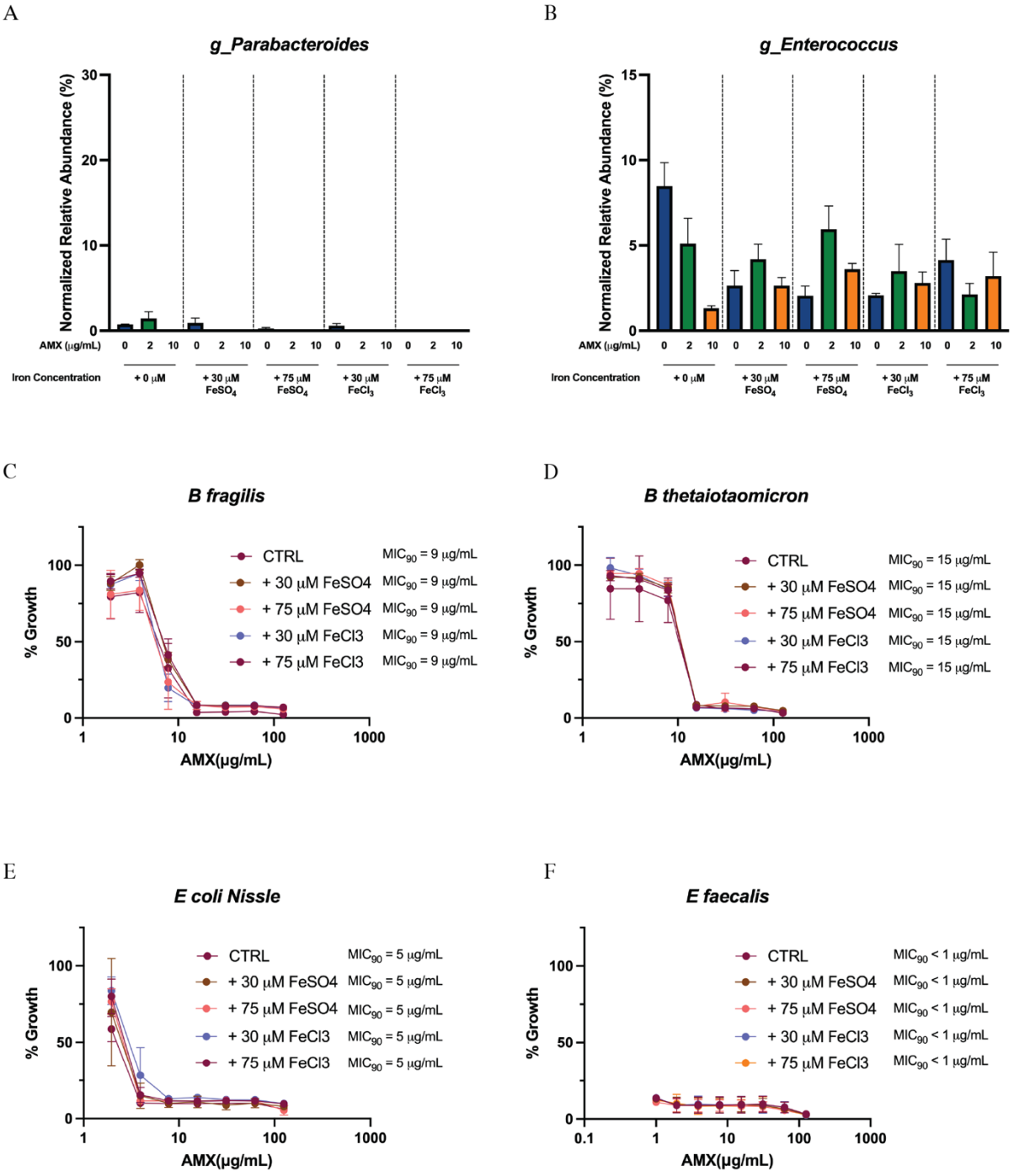

References

1. Berg G, Rybakova D, Fischer D, Cernava T, Vergès MC, Charles T, Chen X, Cocolin L, Eversole K, Corral GH, Kazou M, Kinkel L, Lange L, Lima N, Loy A, Macklin JA, Maguin E, Mauchline T, McClure R, Mitter B, Ryan M, Sarand I, Smidt H, Schelkle B, Roume H, Kiran GS, Selvin J, Souza RSC, van Overbeek L, Singh BK, Wagner M, Walsh A, Sessitsch A, Schloter M. Microbiome definition re-visited: old concepts and new challenges. Microbiome. 2020;8(1):103. Epub 20200630. doi: 10.1186/s40168-020-00875-0. PubMed PMID: 32605663; PMCID: PMC7329523.
2. Hou K, Wu ZX, Chen XY, Wang JQ, Zhang D, Xiao C, Zhu D, Koya JB, Wei L, Li J, Chen ZS. Microbiota in health and diseases. Signal Transduct Target Ther. 2022;7(1):135. Epub 20220423. doi: 10.1038/s41392-022-00974-4. PubMed PMID: 35461318; PMCID: PMC9034083.
3. Thursby E, Juge N. Introduction to the human gut microbiota. Biochem J. 2017;474(11):1823-36. Epub 20170516. doi: 10.1042/bcj20160510. PubMed PMID: 28512250; PMCID: PMC5433529.
4. Rosenberg E. Diversity of bacteria within the human gut and its contribution to the functional unity of holobionts. NPJ Biofilms Microbiomes. 2024;10(1):134. Epub 20241123. doi: 10.1038/s41522-024-00580-y. PubMed PMID: 39580487; PMCID: PMC11585559.
5. Wen L, Duffy A. Factors Influencing the Gut Microbiota, Inflammation, and Type 2 Diabetes. J Nutr. 2017;147(7):1468s-75s. Epub 20170614. doi: 10.3945/jn.116.240754. PubMed PMID: 28615382; PMCID: PMC5483960.
6. Rinninella E, Raoul P, Cintoni M, Franceschi F, Miggiano GAD, Gasbarrini A, Mele MC. What is the Healthy Gut Microbiota Composition? A Changing Ecosystem across Age, Environment, Diet, and Diseases. Microorganisms. 2019;7(1). Epub 20190110. doi: 10.3390/microorganisms7010014. PubMed PMID: 30634578; PMCID: PMC6351938.
7. Rowland I, Gibson G, Heinken A, Scott K, Swann J, Thiele I, Tuohy K. Gut microbiota functions: metabolism of nutrients and other food components. Eur J Nutr. 2018;57(1):1-24. Epub 20170409. doi: 10.1007/s00394-017-1445-8. PubMed PMID: 28393285; PMCID: PMC5847071.
8. Zheng D, Liwinski T, Elinav E. Interaction between microbiota and immunity in health and disease. Cell Res. 2020;30(6):492-506. Epub 20200520. doi: 10.1038/s41422-020-0332-7. PubMed PMID: 32433595; PMCID: PMC7264227.
9. Round JL, Mazmanian SK. The gut microbiota shapes intestinal immune responses during health and disease. Nat Rev Immunol. 2009;9(5):313-23. doi: 10.1038/nri2515. PubMed PMID: 19343057; PMCID: PMC4095778.
10. Lathrop SK, Bloom SM, Rao SM, Nutsch K, Lio CW, Santacruz N, Peterson DA, Stappenbeck TS, Hsieh CS. Peripheral education of the immune system by colonic commensal microbiota. Nature. 2011;478(7368):250-4. Epub 20110921. doi: 10.1038/nature10434. PubMed PMID: 21937990; PMCID: PMC3192908.
11. Kim S, Covington A, Pamer EG. The intestinal microbiota: Antibiotics, colonization resistance, and enteric pathogens. Immunol Rev. 2017;279(1):90-105. doi: 10.1111/imr.12563. PubMed PMID: 28856737; PMCID: PMC6026851.
12. Heinzinger LR, Johnson A, Wurster JI, Nilson R, Penumutchu S, Belenky P. Oxygen and Metabolism: Digesting Determinants of Antibiotic Susceptibility in the Gut. iScience.

2020;23(12):101875. Epub 20201130. doi: 10.1016/j.isci.2020.101875. PubMed PMID: 33354661; PMCID: PMC7744946.
13. Zheng L, Kelly CJ, Colgan SP. Physiologic hypoxia and oxygen homeostasis in the healthy intestine. A Review in the Theme: Cellular Responses to Hypoxia. Am J Physiol Cell Physiol. 2015;309(6):C350-60. Epub 20150715. doi: 10.1152/ajpcell.00191.2015. PubMed PMID: 26179603; PMCID: PMC4572369.
14. Nugent SG, Kumar D, Rampton DS, Evans DF. Intestinal luminal pH in inflammatory bowel disease: possible determinants and implications for therapy with aminosalicylates and other drugs. Gut. 2001;48(4):571-7. doi: 10.1136/gut.48.4.571. PubMed PMID: 11247905; PMCID: PMC1728243.
15. Zheng X, Huang F, Zhao A, Lei S, Zhang Y, Xie G, Chen T, Qu C, Rajani C, Dong B, Li D, Jia W. Bile acid is a significant host factor shaping the gut microbiome of diet-induced obese mice. BMC Biol. 2017;15(1):120. Epub 20171214. doi: 10.1186/s12915-017-0462-7. PubMed PMID: 29241453; PMCID: PMC5731064.
16. Gu S, Chen D, Zhang JN, Lv X, Wang K, Duan LP, Nie Y, Wu XL. Bacterial community mapping of the mouse gastrointestinal tract. PLoS One. 2013;8(10):e74957. Epub 20131007. doi: 10.1371/journal.pone.0074957. PubMed PMID: 24116019; PMCID: PMC3792069.
17. Donaldson GP, Lee SM, Mazmanian SK. Gut biogeography of the bacterial microbiota. Nat Rev Microbiol. 2016;14(1):20-32. Epub 20151026. doi: 10.1038/nrmicro3552. PubMed PMID: 26499895; PMCID: PMC4837114.
18. Zheng L, Kelly CJ, Colgan SP. Physiologic hypoxia and oxygen homeostasis in the healthy intestine. A Review in the Theme: Cellular Responses to Hypoxia. American Journal of Physiology-Cell Physiology. 2015;309(6):C350-C60. doi: 10.1152/ajpcell.00191.2015. PubMed PMID: 26179603.
19. Cummings JH, Macfarlane GT. Role of intestinal bacteria in nutrient metabolism. Clinical Nutrition. 1997;16(1):3-11. doi: https://doi.org/10.1016/S0261-5614(97)80252-X.
20. Krajmalnik-Brown R, Ilhan ZE, Kang DW, DiBaise JK. Effects of gut microbes on nutrient absorption and energy regulation. Nutr Clin Pract. 2012;27(2):201-14. Epub 20120224. doi: 10.1177/0884533611436116. PubMed PMID: 22367888; PMCID: PMC3601187.
21. Weiss GA, Hennet T. Mechanisms and consequences of intestinal dysbiosis. Cellular and Molecular Life Sciences. 2017;74(16):2959-77. doi: 10.1007/s00018-017-2509-x.
22. Hrncir T. Gut Microbiota Dysbiosis: Triggers, Consequences, Diagnostic and Therapeutic Options. Microorganisms. 2022;10(3). Epub 20220307. doi: 10.3390/microorganisms10030578. PubMed PMID: 35336153; PMCID: PMC8954387.
23. Martinez KB, Leone V, Chang EB. Western diets, gut dysbiosis, and metabolic diseases: Are they linked? Gut Microbes. 2017;8(2):130-42. Epub 20170106. doi: 10.1080/19490976.2016.1270811. PubMed PMID: 28059614; PMCID: PMC5390820.
24. Shin N-R, Whon TW, Bae J-W. Proteobacteria: microbial signature of dysbiosis in gut microbiota. Trends in Biotechnology. 2015;33(9):496-503. doi: https://doi.org/10.1016/j.tibtech.2015.06.011.
25. Patangia DV, Anthony Ryan C, Dempsey E, Paul Ross R, Stanton C. Impact of antibiotics on the human microbiome and consequences for host health. Microbiologyopen.

2022;11(1):e1260. doi: 10.1002/mbo3.1260. PubMed PMID: 35212478; PMCID: PMC8756738.
26. Goldenberg JZ, Lytvyn L, Steurich J, Parkin P, Mahant S, Johnston BC. Probiotics for the prevention of pediatric antibiotic-associated diarrhea. Cochrane Database Syst Rev. 2015(12):Cd004827. Epub 20151222. doi: 10.1002/14651858.CD004827.pub4. PubMed PMID: 26695080.
27. Maciel-Fiuza MF, Muller GC, Campos DMS, do Socorro Silva Costa P, Peruzzo J, Bonamigo RR, Veit T, Vianna FSL. Role of gut microbiota in infectious and inflammatory diseases. Front Microbiol. 2023;14:1098386. Epub 20230327. doi: 10.3389/fmicb.2023.1098386. PubMed PMID: 37051522; PMCID: PMC10083300.
28. Minkoff NZ, Aslam S, Medina M, Tanner-Smith EE, Zackular JP, Acra S, Nicholson MR, Imdad A. Fecal microbiota transplantation for the treatment of recurrent Clostridioides difficile (Clostridium difficile). Cochrane Database of Systematic Reviews. 2023(4). doi: 10.1002/14651858.CD013871.pub2. PubMed PMID: CD013871.
29. Reller LB, Weinstein MP, Petti CA. Detection and Identification of Microorganisms by Gene Amplification and Sequencing. Clinical Infectious Diseases. 2007;44(8):1108-14. doi: 10.1086/512818.
30. Thompson LR, Sanders JG, McDonald D, Amir A, Ladau J, Locey KJ, Prill RJ, Tripathi A, Gibbons SM, Ackermann G, Navas-Molina JA, Janssen S, Kopylova E, Vázquez-Baeza Y, González A, Morton JT, Mirarab S, Zech Xu Z, Jiang L, Haroon MF, Kanbar J, Zhu Q, Jin Song S, Kosciolek T, Bokulich NA, Lefler J, Brislawn CJ, Humphrey G, Owens SM, Hampton-Marcell J, Berg-Lyons D, McKenzie V, Fierer N, Fuhrman JA, Clauset A, Stevens RL, Shade A, Pollard KS, Goodwin KD, Jansson JK, Gilbert JA, Knight R. A communal catalogue reveals Earth's multiscale microbial diversity. Nature. 2017;551(7681):457-63. Epub 20171101. doi: 10.1038/nature24621. PubMed PMID: 29088705; PMCID: PMC6192678.
31. Sanabria AM, Janice J, Hjerde E, Simonsen GS, Hanssen A-M. Shotgun-metagenomics based prediction of antibiotic resistance and virulence determinants in Staphylococcus aureus from periprosthetic tissue on blood culture bottles. Scientific Reports. 2021;11(1):20848. doi: 10.1038/s41598-021-00383-7.
32. Quast C, Pruesse E, Yilmaz P, Gerken J, Schweer T, Yarza P, Peplies J, Glöckner FO. The SILVA ribosomal RNA gene database project: improved data processing and web-based tools. Nucleic Acids Res. 2013;41(Database issue):D590-6. Epub 20121128. doi: 10.1093/nar/gks1219. PubMed PMID: 23193283; PMCID: PMC3531112.
33. Durazzi F, Sala C, Castellani G, Manfreda G, Remondini D, De Cesare A. Comparison between 16S rRNA and shotgun sequencing data for the taxonomic characterization of the gut microbiota. Sci Rep. 2021;11(1):3030. Epub 20210204. doi: 10.1038/s41598-021-82726-y. PubMed PMID: 33542369; PMCID: PMC7862389.
34. Xiao T, Zhou W. The third generation sequencing: the advanced approach to genetic diseases. Transl Pediatr. 2020;9(2):163-73. doi: 10.21037/tp.2020.03.06. PubMed PMID: 32477917; PMCID: PMC7237973.
35. Wang Y, Zhao Y, Bollas A, Wang Y, Au KF. Nanopore sequencing technology, bioinformatics and applications. Nature Biotechnology. 2021;39(11):1348-65. doi: 10.1038/s41587-021-01108-x.
36. Tyler AD, Mataseje L, Urfano CJ, Schmidt L, Antonation KS, Mulvey MR, Corbett CR. Evaluation of Oxford Nanopore's MinION Sequencing Device for Microbial Whole

Genome Sequencing Applications. Scientific Reports. 2018;8(1):10931. doi: 10.1038/s41598-018-29334-5.
37. Szoboszlay M, Schramm L, Pinzauti D, Scerri J, Sandionigi A, Biazzo M. Nanopore Is Preferable over Illumina for 16S Amplicon Sequencing of the Gut Microbiota When Species-Level Taxonomic Classification, Accurate Estimation of Richness, or Focus on Rare Taxa Is Required. Microorganisms. 2023;11(3). Epub 20230321. doi: 10.3390/microorganisms11030804. PubMed PMID: 36985377; PMCID: PMC10059749.
38. Workman RE, Tang AD, Tang PS, Jain M, Tyson JR, Razaghi R, Zuzarte PC, Gilpatrick T, Payne A, Quick J, Sadowski N, Holmes N, de Jesus JG, Jones KL, Soulette CM, Snutch TP, Loman N, Paten B, Loose M, Simpson JT, Olsen HE, Brooks AN, Akeson M, Timp W. Nanopore native RNA sequencing of a human poly(A) transcriptome. Nat Methods. 2019;16(12):1297-305. Epub 20191118. doi: 10.1038/s41592-019-0617-2. PubMed PMID: 31740818; PMCID: PMC7768885.
39. Curry KD, Wang Q, Nute MG, Tyshaieva A, Reeves E, Soriano S, Wu Q, Graeber E, Finzer P, Mendling W, Savidge T, Villapol S, Dilthey A, Treangen TJ. Emu: species-level microbial community profiling of full-length 16S rRNA Oxford Nanopore sequencing data. Nat Methods. 2022;19(7):845-53. Epub 20220630. doi: 10.1038/s41592-022-01520-4. PubMed PMID: 35773532; PMCID: PMC9939874.
40. Johns NI, Blazejewski T, Gomes ALC, Wang HH. Principles for designing synthetic microbial communities. Current Opinion in Microbiology. 2016;31:146-53. doi: https://doi.org/10.1016/j.mib.2016.03.010.
41. Weiss AS, Burrichter AG, Durai Raj AC, von Strempel A, Meng C, Kleigrewe K, Münch PC, Rössler L, Huber C, Eisenreich W, Jochum LM, Göing S, Jung K, Lincetto C, Hübner J, Marinos G, Zimmermann J, Kaleta C, Sanchez A, Stecher B. In vitro interaction network of a synthetic gut bacterial community. The ISME Journal. 2022;16(4):1095-109. doi: 10.1038/s41396-021-01153-z.
42. Chen X, Mengxue G, Lina W, Guifen Q, Yili W, He H, and Kang G. A synthetic microbial consortium protects against obesity by regulating vitamin B6 metabolism. Gut Microbes. 2024;16(1):2304901. doi: 10.1080/19490976.2024.2304901.
43. Cheng AG, Ho P-Y, Aranda-Díaz A, Jain S, Yu FB, Meng X, Wang M, Iakiviak M, Nagashima K, Zhao A, Murugkar P, Patil A, Atabakhsh K, Weakley A, Yan J, Brumbaugh AR, Higginbottom S, Dimas A, Shiver AL, Deutschbauer A, Neff N, Sonnenburg JL, Huang KC, Fischbach MA. Design, construction, and in vivo augmentation of a complex gut microbiome. Cell. 2022;185(19):3617-36.e19. doi: https://doi.org/10.1016/j.cell.2022.08.003.
44. Banerjee A, Chatterji U. Prevalence of perturbed gut microbiota in pathophysiology of arsenic-induced anxiety- and depression-like behaviour in mice. Chemosphere. 2024;364:143293. doi: https://doi.org/10.1016/j.chemosphere.2024.143293.
45. Hirano R, Nishita I, Nakai R, Bito A, Sasabe R, Kurihara S. Development of culture methods capable of culturing a wide range of predominant species of intestinal bacteria. Frontiers in Cellular and Infection Microbiology. 2023;13.
46. Tao X, Huang W, Pan L, Sheng L, Qin Y, Chen L, Yu L, Wu G, Wan J, Li H. Optimizing ex vivo culture conditions to study human gut microbiome. ISME Communications. 2023;3(1):38. doi: 10.1038/s43705-023-00245-5.
47. Goodman AL, Kallstrom G, Faith JJ, Reyes A, Moore A, Dantas G, Gordon JI. Extensive personal human gut microbiota culture collections characterized and manipulated in

gnotobiotic mice. Proc Natl Acad Sci U S A. 2011;108(15):6252-7. Epub 20110321. doi: 10.1073/pnas.1102938108. PubMed PMID: 21436049; PMCID: PMC3076821.
48. Aranda-Díaz A, Ng KM, Thomsen T, Real-Ramírez I, Dahan D, Dittmar S, Gonzalez CG, Chavez T, Vasquez KS, Nguyen TH, Yu FB, Higginbottom SK, Neff NF, Elias JE, Sonnenburg JL, Huang KC. Establishment and characterization of stable, diverse, fecal-derived in vitro microbial communities that model the intestinal microbiota. Cell Host Microbe. 2022;30(2):260-72.e5. Epub 20220119. doi: 10.1016/j.chom.2021.12.008. PubMed PMID: 35051349; PMCID: PMC9082339.
49. Celis AI, Relman DA, Huang KC. The impact of iron and heme availability on the healthy human gut microbiome in vivo and in vitro. Cell Chemical Biology. 2023;30(1):110-26.e3. doi: https://doi.org/10.1016/j.chembiol.2022.12.001.
50. Średnicka P, Roszko MŁ, Popowski D, Kowalczyk M, Wójcicki M, Emanowicz P, Szczepańska M, Kotyrba D, Juszczuk-Kubiak E. Effect of in vitro cultivation on human gut microbiota composition using 16S rDNA amplicon sequencing and metabolomics approach. Scientific Reports. 2023;13(1):3026. doi: 10.1038/s41598-023-29637-2.
51. Garcia-Santamarina S, Kuhn M, Devendran S, Maier L, Driessen M, Mateus A, Mastrorilli E, Brochado AR, Savitski MM, Patil KR, Zimmermann M, Bork P, Typas A. Emergence of community behaviors in the gut microbiota upon drug treatment. Cell. 2024;187(22):6346-57.e20. doi: https://doi.org/10.1016/j.cell.2024.08.037.
52. van Bergen LAH, Alonso M, Palló A, Nilsson L, De Proft F, Messens J. Revisiting sulfur H-bonds in proteins: The example of peroxiredoxin AhpE. Scientific Reports. 2016;6(1):30369. doi: 10.1038/srep30369.
53. Lobo IA, Robertson PA, Villani L, Wilson DJD, Robertson EG. Thiols as Hydrogen Bond Acceptors and Donors: Spectroscopy of 2-Phenylethanethiol Complexes. The Journal of Physical Chemistry A. 2018;122(36):7171-80. doi: 10.1021/acs.jpca.8b06649.
54. Prevention CfDCa. Outpatient Antibiotic Prescriptions - United Stated, 20222022.
55. Pankey GA, Sabath LD. Clinical Relevance of Bacteriostatic versus Bactericidal Mechanisms of Action in the Treatment of Gram-Positive Bacterial Infections. Clinical Infectious Diseases. 2004;38(6):864-70. doi: 10.1086/381972.
56. Sidebottom AM. A Brief History of Microbial Study and Techniques for Exploring the Gastrointestinal Microbiome. Clin Colon Rectal Surg. 2023;36(2):98-104. Epub 20230125. doi: 10.1055/s-0042-1760678. PubMed PMID: 36844714; PMCID: PMC9946713.
57. Hutchings MI, Truman AW, Wilkinson B. Antibiotics: past, present and future. Current Opinion in Microbiology. 2019;51:72-80. doi: https://doi.org/10.1016/j.mib.2019.10.008.
58. Krause KM, Serio AW, Kane TR, Connolly LE. Aminoglycosides: An Overview. Cold Spring Harb Perspect Med. 2016;6(6). Epub 20160601. doi: 10.1101/cshperspect.a027029. PubMed PMID: 27252397; PMCID: PMC4888811.
59. Pearson JC, Gillett E, Gadri ND, Dionne B. Tetracyclines, the old and the new: A narrative review. CMI Communications. 2025;2(1):105059. doi: https://doi.org/10.1016/j.cmicom.2025.105059.
60. Butler MS, Hansford KA, Blaskovich MAT, Halai R, Cooper MA. Glycopeptide antibiotics: Back to the future. The Journal of Antibiotics. 2014;67(9):631-44. doi: 10.1038/ja.2014.111.
61. Bui T, Patel P, Preuss CV. Cephalosporins. StatPearls. Treasure Island (FL): StatPearls Publishing

62. Papp-Wallace KM, Endimiani A, Taracila MA, Bonomo RA. Carbapenems: past, present, and future. Antimicrob Agents Chemother. 2011;55(11):4943-60. Epub 20110822. doi: 10.1128/aac.00296-11. PubMed PMID: 21859938; PMCID: PMC3195018.
63. Kardos N, Demain AL. Penicillin: the medicine with the greatest impact on therapeutic outcomes. Applied Microbiology and Biotechnology. 2011;92(4):677-87. doi: 10.1007/s00253-011-3587-6.
64. Pallo-Zimmerman LM, Byron JK, Graves TK. Fluoroquinolones: then and now. Compend Contin Educ Vet. 2010;32(7):E1-9; quiz E. PubMed PMID: 20957609.
65. Huttner A, Bielicki J, Clements MN, Frimodt-Møller N, Muller AE, Paccaud JP, Mouton JW. Oral amoxicillin and amoxicillin–clavulanic acid: properties, indications and usage. Clinical Microbiology and Infection. 2020;26(7):871-9. doi: https://doi.org/10.1016/j.cmi.2019.11.028.
66. Cho H, Uehara T, Bernhardt TG. Beta-lactam antibiotics induce a lethal malfunctioning of the bacterial cell wall synthesis machinery. Cell. 2014;159(6):1300-11. doi: 10.1016/j.cell.2014.11.017. PubMed PMID: 25480295; PMCID: PMC4258230.
67. Matsumoto H, Shiotani A, Graham DY. Current and Future Treatment of Helicobacter pylori Infections. Adv Exp Med Biol. 2019;1149:211-25. doi: 10.1007/5584_2019_367. PubMed PMID: 31016626; PMCID: PMC6918954.
68. Rosenfeld RM, Piccirillo JF, Chandrasekhar SS, Brook I, Ashok Kumar K, Kramper M, Orlandi RR, Palmer JN, Patel ZM, Peters A, Walsh SA, Corrigan MD. Clinical practice guideline (update): adult sinusitis. Otolaryngol Head Neck Surg. 2015;152(2 Suppl):S1-s39. doi: 10.1177/0194599815572097. PubMed PMID: 25832968.
69. Chow AW, Benninger MS, Brook I, Brozek JL, Goldstein EJ, Hicks LA, Pankey GA, Seleznick M, Volturo G, Wald ER, File TM, Jr. IDSA clinical practice guideline for acute bacterial rhinosinusitis in children and adults. Clin Infect Dis. 2012;54(8):e72-e112. Epub 20120320. doi: 10.1093/cid/cir1043. PubMed PMID: 22438350.
70. Sartelli M, Guirao X, Hardcastle TC, Kluger Y, Boermeester MA, Raşa K, Ansaloni L, Coccolini F, Montravers P, Abu-Zidan FM, Bartoletti M, Bassetti M, Ben-Ishay O, Biffl WL, Chiara O, Chiarugi M, Coimbra R, De Rosa FG, De Simone B, Di Saverio S, Giannella M, Gkiokas G, Khokha V, Labricciosa FM, Leppäniemi A, Litvin A, Moore EE, Negoi I, Pagani L, Peghin M, Picetti E, Pintar T, Pupelis G, Rubio-Perez I, Sakakushev B, Segovia-Lohse H, Sganga G, Shelat V, Sugrue M, Tarasconi A, Tranà C, Ulrych J, Viale P, Catena F. 2018 WSES/SIS-E consensus conference: recommendations for the management of skin and soft-tissue infections. World J Emerg Surg. 2018;13:58. Epub 20181214. doi: 10.1186/s13017-018-0219-9. PubMed PMID: 30564282; PMCID: PMC6295010.
71. Tan CW, Chlebicki MP. Urinary tract infections in adults. Singapore Med J. 2016;57(9):485-90. doi: 10.11622/smedj.2016153. PubMed PMID: 27662890; PMCID: PMC5027397.
72. Shulman ST, Bisno AL, Clegg HW, Gerber MA, Kaplan EL, Lee G, Martin JM, Van Beneden C. Clinical practice guideline for the diagnosis and management of group A streptococcal pharyngitis: 2012 update by the Infectious Diseases Society of America. Clin Infect Dis. 2012;55(10):e86-102. Epub 20120909. doi: 10.1093/cid/cis629. PubMed PMID: 22965026; PMCID: PMC7108032.

73. Walsh TR, Gales AC, Laxminarayan R, Dodd PC. Antimicrobial Resistance: Addressing a Global Threat to Humanity. PLoS Med. 2023;20(7):e1004264. Epub 20230703. doi: 10.1371/journal.pmed.1004264. PubMed PMID: 37399216; PMCID: PMC10317217.
74. Lobritz MA, Belenky P, Porter CBM, Gutierrez A, Yang JH, Schwarz EG, Dwyer DJ, Khalil AS, Collins JJ. Antibiotic efficacy is linked to bacterial cellular respiration. Proceedings of the National Academy of Sciences. 2015;112(27):8173-80. doi: 10.1073/pnas.1509743112.
75. Belenky P, Ye Jonathan D, Porter Caroline BM, Cohen Nadia R, Lobritz Michael A, Ferrante T, Jain S, Korry Benjamin J, Schwarz Eric G, Walker Graham C, Collins James J. Bactericidal Antibiotics Induce Toxic Metabolic Perturbations that Lead to Cellular Damage. Cell Reports. 2015;13(5):968-80. doi: 10.1016/j.celrep.2015.09.059.
76. Cabral DJ, Penumutchu S, Reinhart EM, Zhang C, Korry BJ, Wurster JI, Nilson R, Guang A, Sano WH, Rowan-Nash AD, Li H, Belenky P. Microbial Metabolism Modulates Antibiotic Susceptibility within the Murine Gut Microbiome. Cell Metab. 2019;30(4):800-23.e7. Epub 20190912. doi: 10.1016/j.cmet.2019.08.020. PubMed PMID: 31523007; PMCID: PMC6948150.
77. Nilson R, Penumutchu S, Pagano FS, Belenky P. Metabolic changes associated with polysaccharide utilization reduce susceptibility to some β-lactams in Bacteroides thetaiotaomicron. mSphere. 2024;9(8):e0010324. Epub 20240807. doi: 10.1128/msphere.00103-24. PubMed PMID: 39109911; PMCID: PMC11351048.
78. Penumutchu S, Korry BJ, Hewlett K, Belenky P. Fiber supplementation protects from antibiotic-induced gut microbiome dysbiosis by modulating gut redox potential. Nat Commun. 2023;14(1):5161. Epub 20230824. doi: 10.1038/s41467-023-40553-x. PubMed PMID: 37620319; PMCID: PMC10449846.
79. Py B, Barras F. Building Fe-S proteins: bacterial strategies. Nat Rev Microbiol. 2010;8(6):436-46. doi: 10.1038/nrmicro2356. PubMed PMID: 20467446.
80. Sawicki KT, Chang HC, Ardehali H. Role of heme in cardiovascular physiology and disease. J Am Heart Assoc. 2015;4(1):e001138. Epub 20150105. doi: 10.1161/jaha.114.001138. PubMed PMID: 25559010; PMCID: PMC4330050.
81. Rachmilovich-Calis S, Masarwa A, Meyerstein N, Meyerstein D, van Eldik R. New Mechanistic Aspects of the Fenton Reaction. Chemistry – A European Journal. 2009;15(33):8303-9. doi: https://doi.org/10.1002/chem.200802572.
82. Ranji-Burachaloo H, Gurr PA, Dunstan DE, Qiao GG. Cancer Treatment through Nanoparticle-Facilitated Fenton Reaction. ACS Nano. 2018;12(12):11819-37. doi: 10.1021/acsnano.8b07635.
83. Cadet J, Douki T, Ravanat JL. Oxidatively generated base damage to cellular DNA. Free Radic Biol Med. 2010;49(1):9-21. Epub 20100402. doi: 10.1016/j.freeradbiomed.2010.03.025. PubMed PMID: 20363317.
84. Sheng H, Nakamura K, Kanno T, Sasaki K, Niwano Y, editors. Microbicidal Activity of Artificially Generated Hydroxyl Radicals2015; Tokyo: Springer Japan.
85. Merino C, Kuzyakov Y, Godoy K, Cornejo P, Matus F. Synergy effect of peroxidase enzymes and Fenton reactions greatly increase the anaerobic oxidation of soil organic matter. Scientific Reports. 2020;10(1):11289. doi: 10.1038/s41598-020-67953-z.
86. Liu T, Chen D, Li X, Li F. Microbially mediated coupling of nitrate reduction and Fe(II) oxidation under anoxic conditions. FEMS Microbiology Ecology. 2019;95(4). doi: 10.1093/femsec/fiz030.

87. Kashefi K, Holmes DE, Reysenbach AL, Lovley DR. Use of Fe(III) as an electron acceptor to recover previously uncultured hyperthermophiles: isolation and characterization of Geothermobacterium ferrireducens gen. nov., sp. nov. Appl Environ Microbiol. 2002;68(4):1735-42. doi: 10.1128/aem.68.4.1735-1742.2002. PubMed PMID: 11916691; PMCID: PMC123901.
88. Nealson KH, Saffarini D. Iron and manganese in anaerobic respiration: environmental significance, physiology, and regulation. Annu Rev Microbiol. 1994;48:311-43. doi: 10.1146/annurev.mi.48.100194.001523. PubMed PMID: 7826009.
89. Ezraty B, Barras F. The 'liaisons dangereuses' between iron and antibiotics. FEMS Microbiology Reviews. 2016;40(3):418-35. doi: 10.1093/femsre/fuw004.
90. Mochizuki H, Yamada H, Oikawa Y, Murakami K, Ishiguro J, Kosuzume H, Aizawa N, Mochida E. Bactericidal activity of M14659 enhanced in low-iron environments. Antimicrobial Agents and Chemotherapy. 1988;32(11):1648-54. doi: 10.1128/aac.32.11.1648.
91. Kohanski MA, Dwyer DJ, Hayete B, Lawrence CA, Collins JJ. A Common Mechanism of Cellular Death Induced by Bactericidal Antibiotics. Cell. 2007;130(5):797-810. doi: https://doi.org/10.1016/j.cell.2007.06.049.
92. Wang X, Zhao X. Contribution of Oxidative Damage to Antimicrobial Lethality. Antimicrobial Agents and Chemotherapy. 2009;53(4):1395-402. doi: 10.1128/aac.01087-08.
93. Liu Y, Imlay JA. Cell death from antibiotics without the involvement of reactive oxygen species. Science. 2013;339(6124):1210-3. doi: 10.1126/science.1232751. PubMed PMID: 23471409; PMCID: PMC3731989.
94. Ma L, Gao Y, Maresso AW. Escherichia coli Free Radical-Based Killing Mechanism Driven by a Unique Combination of Iron Restriction and Certain Antibiotics. J Bacteriol. 2015;197(23):3708-19. Epub 20150921. doi: 10.1128/jb.00758-15. PubMed PMID: 26391205; PMCID: PMC4626890.
95. Yeom J, Imlay JA, Park W. Iron homeostasis affects antibiotic-mediated cell death in Pseudomonas species. J Biol Chem. 2010;285(29):22689-95. Epub 20100517. doi: 10.1074/jbc.M110.127456. PubMed PMID: 20479007; PMCID: PMC2903419.
96. Kreamer Naomi N, Costa F, Newman Dianne K. The Ferrous Iron-Responsive BqsRS Two-Component System Activates Genes That Promote Cationic Stress Tolerance. mBio. 2015;6(2):10.1128/mbio.02549-14. doi: 10.1128/mbio.02549-14.
97. Oglesby-Sherrouse AG, Djapgne L, Nguyen AT, Vasil AI, Vasil ML. The complex interplay of iron, biofilm formation, and mucoidy affecting antimicrobial resistance of Pseudomonas aeruginosa. Pathog Dis. 2014;70(3):307-20. Epub 20140210. doi: 10.1111/2049-632x.12132. PubMed PMID: 24436170; PMCID: PMC4084922.
98. Cuisiniere T, Calvé A, Fragoso G, Oliero M, Hajjar R, Gonzalez E, Santos MM. Oral iron supplementation after antibiotic exposure induces a deleterious recovery of the gut microbiota. BMC Microbiology. 2021;21(1):259. doi: 10.1186/s12866-021-02320-0.
99. DSMZ. 63: Desulfovibrio (Postgate) Medium.
100. McMurdie PJ, Holmes S. phyloseq: an R package for reproducible interactive analysis and graphics of microbiome census data. PLoS One. 2013;8(4):e61217. Epub 20130422. doi: 10.1371/journal.pone.0061217. PubMed PMID: 23630581; PMCID: PMC3632530.

101. Lozupone C, Knight R. UniFrac: a new phylogenetic method for comparing microbial communities. Appl Environ Microbiol. 2005;71(12):8228-35. doi: 10.1128/aem.71.12.8228-8235.2005. PubMed PMID: 16332807; PMCID: PMC1317376.
102. Mallick H, Rahnavard A, McIver LJ, Ma S, Zhang Y, Nguyen LH, Tickle TL, Weingart G, Ren B, Schwager EH, Chatterjee S, Thompson KN, Wilkinson JE, Subramanian A, Lu Y, Waldron L, Paulson JN, Franzosa EA, Bravo HC, Huttenhower C. Multivariable association discovery in population-scale meta-omics studies. PLoS Comput Biol. 2021;17(11):e1009442. Epub 20211116. doi: 10.1371/journal.pcbi.1009442. PubMed PMID: 34784344; PMCID: PMC8714082.
103. Richter K, Schicklberger M, Gescher J. Dissimilatory reduction of extracellular electron acceptors in anaerobic respiration. Appl Environ Microbiol. 2012;78(4):913-21. Epub 20111216. doi: 10.1128/aem.06803-11. PubMed PMID: 22179232; PMCID: PMC3273014.
104. Hess SY, Owais A, Jefferds MED, Young MF, Cahill A, Rogers LM. Accelerating action to reduce anemia: Review of causes and risk factors and related data needs. Annals of the New York Academy of Sciences. 2023;1523(1):11-23. doi: https://doi.org/10.1111/nyas.14985.
105. Wexler HM. Bacteroides: the good, the bad, and the nitty-gritty. Clin Microbiol Rev. 2007;20(4):593-621. doi: 10.1128/cmr.00008-07. PubMed PMID: 17934076; PMCID: PMC2176045.
106. Zafar H, Saier MH, Jr. Gut Bacteroides species in health and disease. Gut Microbes. 2021;13(1):1-20. doi: 10.1080/19490976.2020.1848158. PubMed PMID: 33535896; PMCID: PMC7872030.
107. Comstock LE, Coyne MJ. Bacteroides thetaiotaomicron: a dynamic, niche-adapted human symbiont. Bioessays. 2003;25(10):926-9. doi: 10.1002/bies.10350. PubMed PMID: 14505359.
108. Brook I. Spectrum and treatment of anaerobic infections. J Infect Chemother. 2016;22(1):1-13. Epub 20151124. doi: 10.1016/j.jiac.2015.10.010. PubMed PMID: 26620376.
109. Spiga L, Fansler RT, Perera YR, Shealy NG, Munneke MJ, David HE, Torres TP, Lemoff A, Ran X, Richardson KL, Pudlo N, Martens EC, Folta-Stogniew E, Yang ZJ, Skaar EP, Byndloss MX, Chazin WJ, Zhu W. Iron acquisition by a commensal bacterium modifies host nutritional immunity during Salmonella infection. Cell Host & Microbe. 2023;31(10):1639-54.e10. doi: https://doi.org/10.1016/j.chom.2023.08.018.
110. Rocha ER, Bergonia HA, Gerdes S, Jeffrey Smith C. Bacteroides fragilis requires the ferrous-iron transporter FeoAB and the CobN-like proteins BtuS1 and BtuS2 for assimilation of iron released from heme. Microbiologyopen. 2019;8(4):e00669. Epub 20180621. doi: 10.1002/mbo3.669. PubMed PMID: 29931811; PMCID: PMC6460266.
111. Hibbing ME, Fuqua C, Parsek MR, Peterson SB. Bacterial competition: surviving and thriving in the microbial jungle. Nat Rev Microbiol. 2010;8(1):15-25. doi: 10.1038/nrmicro2259. PubMed PMID: 19946288; PMCID: PMC2879262.
112. Veeranagouda Y, Husain F, Boente R, Moore J, Smith CJ, Rocha ER, Patrick S, Wexler HM. Deficiency of the ferrous iron transporter FeoAB is linked with metronidazole resistance in Bacteroides fragilis. Journal of Antimicrobial Chemotherapy. 2014;69(10):2634-43. doi: 10.1093/jac/dku219.

113. Meslé Margaux M, Gray Chase R, Dlakić M, DuBois Jennifer L. Bacteroides thetaiotaomicron, a Model Gastrointestinal Tract Species, Prefers Heme as an Iron Source, Yields Protoporphyrin IX as a Product, and Acts as a Heme Reservoir. Microbiology Spectrum. 2023;11(2):e04815-22. doi: 10.1128/spectrum.04815-22.
114. Ju T, Kong JY, Stothard P, Willing BP. Defining the role of Parasutterella, a previously uncharacterized member of the core gut microbiota. The ISME Journal. 2019;13(6):1520-34. doi: 10.1038/s41396-019-0364-5.
115. Chiodini RJ, Dowd SE, Chamberlin WM, Galandiuk S, Davis B, Glassing A. Microbial Population Differentials between Mucosal and Submucosal Intestinal Tissues in Advanced Crohn's Disease of the Ileum. PLoS One. 2015;10(7):e0134382. Epub 20150729. doi: 10.1371/journal.pone.0134382. PubMed PMID: 26222621; PMCID: PMC4519195.
116. Blasco-Baque V, Coupé B, Fabre A, Handgraaf S, Gourdy P, Arnal JF, Courtney M, Schuster-Klein C, Guardiola B, Tercé F, Burcelin R, Serino M. Associations between hepatic miRNA expression, liver triacylglycerols and gut microbiota during metabolic adaptation to high-fat diet in mice. Diabetologia. 2017;60(4):690-700. Epub 20170119. doi: 10.1007/s00125-017-4209-3. PubMed PMID: 28105518; PMCID: PMC6518927.
117. Chen Y-J, Wu H, Wu S-D, Lu N, Wang Y-T, Liu H-N, Dong L, Liu T-T, Shen X-Z. Parasutterella, in association with irritable bowel syndrome and intestinal chronic inflammation. Journal of Gastroenterology and Hepatology. 2018;33(11):1844-52. doi: https://doi.org/10.1111/jgh.14281.
118. Sóki J, Wybo I, Baaity Z, Stefán G, Jeverica S, Ulger N, Stingu CS, Mahmood B, Burián K, Nagy E. Detection of the antibiotic resistance genes content of intestinal Bacteroides, Parabacteroides and Phocaeicola isolates from healthy and carbapenem-treated patients from European countries. BMC Microbiol. 2024;24(1):202. Epub 20240608. doi: 10.1186/s12866-024-03354-w. PubMed PMID: 38851699; PMCID: PMC11162026.
119. Choi JS, Seok YJ, Cho YH, Roe JH. Iron-Induced Respiration Promotes Antibiotic Resistance in Actinomycete Bacteria. mBio. 2022;13(2):e0042522. Epub 20220331. doi: 10.1128/mbio.00425-22. PubMed PMID: 35357210; PMCID: PMC9040825.
120. Singha S, Thomas R, Viswakarma JN, Gupta VK. Foodborne illnesses of Escherichia coli O157origin and its control measures. J Food Sci Technol. 2023;60(4):1274-83. Epub 20220207. doi: 10.1007/s13197-022-05381-9. PubMed PMID: 36936116; PMCID: PMC10020406.
121. Zaidi MB, Estrada-García T. Shigella: A Highly Virulent and Elusive Pathogen. Curr Trop Med Rep. 2014;1(2):81-7. doi: 10.1007/s40475-014-0019-6. PubMed PMID: 25110633; PMCID: PMC4126259.
122. Scaldaferri F, Gerardi V, Mangiola F, Lopetuso LR, Pizzoferrato M, Petito V, Papa A, Stojanovic J, Poscia A, Cammarota G, Gasbarrini A. Role and mechanisms of action of Escherichia coli Nissle 1917 in the maintenance of remission in ulcerative colitis patients: An update. World J Gastroenterol. 2016;22(24):5505-11. doi: 10.3748/wjg.v22.i24.5505. PubMed PMID: 27350728; PMCID: PMC4917610.
123. Michels KR, Lambrecht NJ, Carson WF, Schaller MA, Lukacs NW, Bermick JR. The Role of Iron in the Susceptibility of Neonatal Mice to Escherichia coli K1 Sepsis. J Infect Dis. 2019;220(7):1219-29. doi: 10.1093/infdis/jiz282. PubMed PMID: 31136646; PMCID: PMC7325330.

124. Telang S, Vimr E, Mahoney JR, Law I, Lundqvist-Gustafsson H, Qian M, Eaton JW. Strain-Specific Iron-Dependent Virulence in Escherichia coli. The Journal of Infectious Diseases. 2001;184(2):159-65. doi: 10.1086/322017.
125. Li C-J, Zhang Z, Zhan P-C, Lv A-P, Li P-P, Liu L, Li W-J, Yang L-L, Zhi X-Y. Comparative genomic analysis and proposal of Clostridium yunnanense sp. nov., Clostridium rhizosphaerae sp. nov., and Clostridium paridis sp. nov., three novel Clostridium sensu stricto endophytes with diverse capabilities of acetic acid and ethanol production. Anaerobe. 2023;79:102686. doi: https://doi.org/10.1016/j.anaerobe.2022.102686.
126. Peck MW, van Vliet AHM. Impact of Clostridium botulinum genomic diversity on food safety. Current Opinion in Food Science. 2016;10:52-9. doi: https://doi.org/10.1016/j.cofs.2016.09.006.
127. Garrigues L, Do TD, Bideaux C, Guillouet SE, Meynial-Salles I. Insights into Clostridium tetani: From genome to bioreactors. Biotechnology Advances. 2022;54:107781. doi: https://doi.org/10.1016/j.biotechadv.2021.107781.
128. Cassir N, Benamar S, La Scola B. Clostridium butyricum: from beneficial to a new emerging pathogen. Clinical Microbiology and Infection. 2016;22(1):37-45. doi: https://doi.org/10.1016/j.cmi.2015.10.014.
129. Fenicia L, Anniballi F, Aureli P. Intestinal toxemia botulism in Italy, 1984–2005. European Journal of Clinical Microbiology & Infectious Diseases. 2007;26(6):385-94. doi: 10.1007/s10096-007-0301-9.
130. Vazquez-Gutierrez P, de Wouters T, Werder J, Chassard C, Lacroix C. High Iron-Sequestrating Bifidobacteria Inhibit Enteropathogen Growth and Adhesion to Intestinal Epithelial Cells In vitro. Frontiers in Microbiology. 2016;Volume 7 - 2016. doi: 10.3389/fmicb.2016.01480.
131. Vazquez-Gutierrez P, Stevens MJA, Gehrig P, Barkow-Oesterreicher S, Lacroix C, Chassard C. The extracellular proteome of two Bifidobacterium species reveals different adaptation strategies to low iron conditions. BMC Genomics. 2017;18(1):41. doi: 10.1186/s12864-016-3472-x.
132. Su C, Zhang M, Lin L, Yu G, Zhong H, Chong Y. Reduction of iron oxides and microbial community composition in iron-rich soils with different organic carbon as electron donors. International Biodeterioration & Biodegradation. 2020;148:104881. doi: https://doi.org/10.1016/j.ibiod.2019.104881.
133. Gräff ÁT, Barry SM. Siderophores as tools and treatments. npj Antimicrobials and Resistance. 2024;2(1):47. doi: 10.1038/s44259-024-00053-4.
134. Smith AD, Wilks A. Chapter Thirteen - Extracellular Heme Uptake and the Challenges of Bacterial Cell Membranes. In: Argüello JM, Lutsenko S, editors. Current Topics in Membranes: Academic Press; 2012. p. 359-92.
135. Contreras H, Chim N, Credali A, Goulding CW. Heme uptake in bacterial pathogens. Curr Opin Chem Biol. 2014;19:34-41. Epub 20140104. doi: 10.1016/j.cbpa.2013.12.014. PubMed PMID: 24780277; PMCID: PMC4007353.
136. Cavas L, Kirkiz I. Characterization of siderophores from Escherichia coli strains through genome mining tools: an antiSMASH study. AMB Express. 2022;12(1):74. Epub 20220615. doi: 10.1186/s13568-022-01421-x. PubMed PMID: 35704153; PMCID: PMC9200922.

137. Gao Q, Wang X, Xu H, Xu Y, Ling J, Zhang D, Gao S, Liu X. Roles of iron acquisition systems in virulence of extraintestinal pathogenic Escherichia coli: salmochelin and aerobactin contribute more to virulence than heme in a chicken infection model. BMC Microbiol. 2012;12:143. Epub 20120720. doi: 10.1186/1471-2180-12-143. PubMed PMID: 22817680; PMCID: PMC3496646.
138. Courcelle J, Hanawalt PC. RecA-Dependent Recovery of Arrested DNA Replication Forks. Annual Review of Genetics. 2003;37(Volume 37, 2003):611-46. doi: https://doi.org/10.1146/annurev.genet.37.110801.142616.
139. Cory MB, Li A, Hurley CM, Carman PJ, Pumroy RA, Hostetler ZM, Perez RM, Venkatesh Y, Li X, Gupta K, Petersson EJ, Kohli RM. The LexA–RecA* structure reveals a cryptic lock-and-key mechanism for SOS activation. Nature Structural & Molecular Biology. 2024;31(10):1522-31. doi: 10.1038/s41594-024-01317-3.